HHS Public Access

Author manuscript

Biochemistry. Author manuscript; available in PMC 2019 June 19.

Published in final edited form as:

Biochemistry. 2018 June 19; 57(24): 3309–3325. doi:10.1021/acs.biochem.8b00239.

Mini-Review: Ergothioneine and Ovothiol Biosyntheses, an Unprecedented Trans-Sulfur Strategy in Natural Product Biosynthesis

Nathchar Naowarojna[†], **Ronghai Cheng**[†], **Li Chen**[†,‡], **Melissa Quill**[†], **Meiling Xu**[†], **Changming Zhao**[†,‡,*], and **Pinghua Liu**[†,*]

[†]Department of Chemistry, Boston University, Boston, Massachusetts 02215, United States

[‡]Key Laboratory of Combinatory Biosynthesis and Drug Discovery, Ministry of Education, School of Pharmaceutical Sciences, Wuhan University, Wuhan, Hubei 430072, People's Republic of China

Abstract

As one of the most abundant elements on earth, sulfur is part of many small molecular metabolites and is key to their biological activities. Over the past few decades, some general strategies have been discovered for the incorporation of sulfur into natural products. In this review, we summarize recent efforts in elucidating the biosynthetic details for two sulfur-containing metabolites, ergothioneine and ovothiol. Their biosyntheses involve an unprecedented trans-sulfur strategy, a combination of a mononuclear non-heme iron enzyme-catalyzed oxidative C–S bond formation reaction and a PLP enzyme-mediated C–S lyase reaction.

Graphical Abstract

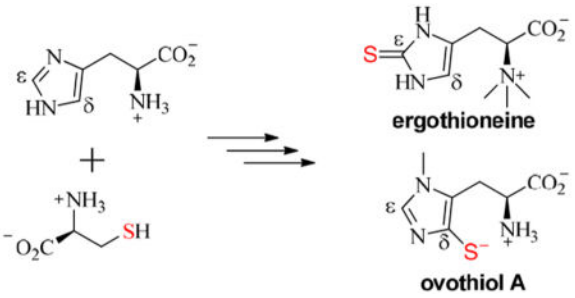

Sulfur is a component of both small molecular metabolites and macromolecules,[1–3] and the roles of sulfur in primary metabolism are well-established.[4–8] Over the past few decades, studies of sulfur-containing vitamins/cofactors (e.g., thiamin pyrophosphate,[9,10] biotin,

*Corresponding Authors: pinghua@bu.edu., cmzhao03@whu.edu.cn.

Author Contributions

N.N., R.C., and L.C., contributed equally to this work.

ORCID

Pinghua Liu: 0000-0002-9768-559X

Notes

The authors declare no competing financial interest.

[9,11–14] lipoic acid,[15] molybdopterin,[16] coenzyme B,[17] and coenzyme M[18,19]) have greatly enriched our understanding on the biosynthetic C–S bond construction strategies. In recent years, an explosion of genetic information from genome sequencing efforts revealed many potential sulfur-containing natural product biosynthetic gene clusters.[20–23] Currently known enzymatic C–S bond formation reactions can be roughly divided into two categories: ionic mechanisms and radical mechanisms.

Ionic Types of C–S Bond Formation Biosynthetic Pathways

The pK_a of cysteine thiol is ~8.3, and under physiological conditions (e.g., pH 7.4), a portion of the cysteine side chain is present as a thiolate, which could function as a nucleophile directly. In nisin **1** biosynthesis (Figure 1A),[24] an example of lantibiotic biosynthesis,[25] thioether bond formation involves several steps. The serine and threonine residues are dehydrated by NisB, resulting in a 2,3-didehydroalanine (Dha) or 2,3-didehydrobutyrine (Dhb) moiety (Figure 1A). A Zn^{2+}-containing cyclase, NisC, catalyzes the nucleophilic attacks on the β-carbon position of Dhb or Dha by cysteine residues, producing thioether linkages. In the NisC reaction, the coordination of a cysteine residue to Zn^{2+} decreases its pK_a, facilitating thioether bond formation (Figure 1B).[24] In the last step, a protease, NisP, cleaves off the leader peptide from the thioether-containing peptide to give nisin **1** as the final product (Figure 1A).

In some cases, electrophiles for the nucleophilic reactions are created by oxidative activation mechanisms. Several types of oxidases have been reported to be part of this type of activation mechanism, including P450 monooxygenases, non-heme iron enzymes, flavin-dependent enzymes, and copper-containing oxidases.[20] This strategy is present in the biosyntheses of gliotoxin [**12** (Figure 2)],[26,27] leukotriene D4,[28,29] and glucosinolate.[30] In gliotoxin **12** biosynthesis, a nonribosomal peptide synthetase, GliP, catalyzes the condensation between L-Ser **2** and L-Phe **3** to cyclo-phenylalanyl-Ser **4** (Figure 2). Hydroxyl groups are incorporated into the α-positions of **4** by a P450-catalyzed hydroxylation (GliC catalysis). The subsequent dehydration reaction of **5** produces an electrophilic acyliminium intermediate **5a**, which then reacts with glutathione to form the C–S bonds in bis-glutathionylated intermediate **6** (GliG catalysis). Then, a γ-glutamyl-transferase, GliK, cleaves the isopeptide bond, and the resulting Cys–Gly dipeptide bond in compound **7** is hydrolyzed by a metal-dependent dipeptidase, GliJ. A PLP-dependent C–S lyase, GliI, finishes the sulfur transfer process to produce the epidithiol **9**. The disulfide bridge in gliotoxin **12** is formed by a flavin-dependent oxidase [GliT, **11** → **12** conversion (Figure 2)].[27,31,32]

In many other ionic sulfur transfer reactions, sulfur atoms are first activated into a persulfide (R-S-SH)[33] or a thiocarboxylate intermediate (R-CO-SH).[4,34,35] Biosyntheses of sulfur-containing cofactors (e.g., thiamine pyrophosphate[10] and molybdopter-in[16]), and the tRNA modification reaction,[9,36] provide mechanistic details about this type of transformation. These two intermediates were also proposed in several secondary metabolite biosynthetic pathways, including BE-7585A,[37] thioquinolobactin,[38,39] thiolactomycin,[40–42] and 6-thiogua-nine.[43,44] The recently reported biosynthetic details for a thiosugar [BE-7585A, **15** (Figure 3)] are consistent with the findings of studies of sulfur-containing cofactors, while

some unique features were uncovered.[37] In the BE-7585A biosynthetic gene cluster, the *BexX* gene is homologous to the thiazole synthase *thiG* gene in thiamine biosynthesis.[9,10,45] The covalent adduct between BexX and the glucose 6-phosphate-derived 2-ketosugar has been confirmed biochemically[45] [**13a** (Figure 3)], and the crystal structure of the BexX–substrate complex has also been reported.[37] Results from biochemical and structural studies support the mechanistic similarities between BexX in BE-7585A biosynthesis and ThiG in thiamine biosynthesis.[37,45]

Interestingly, the BE-7585A biosynthetic gene cluster does not contain any cysteine desulfurases, sulfur carrier proteins, or rhodanese-like proteins. These proteins are required for efficient transfer of the cysteine sulfur to BexX–substrate complex **13a**, if the sulfur transfer strategy, described above, discovered in the biosynthesis of sulfur-containing cofactors is followed in BexX-catalysis. This observation raises the question of what sulfur-delivery machinery is employed by BexX. The genome of the BE-7585A-producing strain, *Amycolatopsis orientalis*, contains five cysteine desulfurase homologues, four sulfur carrier protein homologues (ThiS, MoaD, CysO, and MoaD2), and five rhodanese homologues. The *thiS*, *moaD*, and *cysO* genes are part of the thiamine, molybdopterin, and cysteine biosynthetic gene clusters, respectively, while *moaD2* is a stand-alone gene without clear association with any biosynthetic pathway. Moreover, the thiamine, molybdopterin, and cysteine biosynthetic gene clusters do not encode the enzyme responsible for activating the sulfur carrier proteins (SCPs). In the genome, there is a MoeZ gene whose N-terminus is homologous to ThiF, an activating enzyme in thiamine biosynthesis. The C-terminus of MoeZ has a rhodanese domain. MoeZ can catalyze the activation of both MoaD2 and CysO to produce the thiocarboxylate intermediate at the C-termini of these SCPs (Figure 3). In addition, the C-terminal rhodanese domain of MoeZ mobilizes the sulfur atom into the activated SCP (e.g., CysO or MoaD2), from which sulfur is transferred to the BexX–substrate complex [**13a** → **14** conversions (Figure 3)].[37] This study demonstrated that the sulfur-delivery system (e.g., desulfurases, sulfur carrier proteins, and their activating enzymes) may not be located in a particular secondary metabolite biosynthetic gene cluster. Instead, the sulfur transfer system can be used for multiple pathways, including both primary and secondary metabolism.

Radical Types of C–S Bond Formation Biosynthetic Pathways

Radical-type C–S bond formation chemistries include two major subcategories:[18] anaerobic and aerobic reactions. Biotin synthase, lipoate synthase (anaerobic radical type), and isopenicillin *N*-synthase (IPNS) (aerobic radical type) are well-known examples. Biotin synthase is a radical SAM enzyme,[46] and the reduction of *S*-adenosylmethionine (SAM, **16**) by a [4Fe-4S] cluster leads to the formation of L-Met **17** and 5′-deoxyadenosyl radical (**18**, 5′-dAdo•), which abstracts a hydrogen from the substrate to produce a substrate-based radical [**19a** (Figure 4B)]; this is followed by a sulfur insertion using an auxiliary [2Fe-2S] cluster in BioB as the sulfur source [**19b** → **19c** (Figure 4)].[11,12,15,18] The process is repeated one more time to form the thioether bond in biotin [**19d** → **20** conversion (Figure 4B)].

A similar process is also observed in the *Escherichia coli* lipoic acid biosynthetic pathway (Figure 5). In this pathway, an octanoyltransferase (LipB) first transfers an *n*-octanoyl moiety **21** to a conserved lysine residue on lipoyl carrier protein [**22** (Figure 5)]. Then, a lipoyl synthase, LipA, mediates the sulfur transfer. Like other radical SAM enzymes, the first [4Fe-4S] cluster of LipA undergoes reductive cleavage of SAM to produce 5′-dAdo• [**16** → **18** conversion (Figure 4)], which then abstracts a hydrogen atom from the C_6 position of the substrate to form a substrate-based radical **22a** (Figure 5).[46] The substrate-based radical reacts with the bridging μ-sulfido ion of the auxiliary [4Fe-4S] cluster, while one of the Fe^{3+} ions is reduced to Fe^{2+} and released from the iron–sulfur cluster, resulting in intermediate **22b**. The cycle is repeated one more time to incorporate the other sulfur into the C_8 position of the octanoyl moiety to produce **22d**. In this mechanism, LipA also functions as the sulfur source and supports only a single turnover. Determining how the iron–sulfur cluster is regenerated to support catalytic turnovers has been a challenge for decades. Recently, Booker et al. demonstrated that in *E. coli*, when iron–sulfur cluster carrier protein IscU or Nfu is included in the reaction, LipA can catalyze multiple turnovers. In this case, Nfu or IscU replenishes the auxiliary [4Fe-4S] cluster of LipA to support multiple turnovers.[47,48]

In addition to the aforementioned cases, another type of radical SAM enzyme-mediated C–S bond formation strategy has been reported recently (Figure 6). In sactipeptides, one subclass of ribosomally synthesized and post-translationally modified peptides (RiPP),[20,49] there are also thioether linkages. However, different from lantibiotics discussed in Figure 1, the thioether linkage in sactipeptides is formed between a cysteine sulfur atom and the α-carbon, instead of the β-carbon of another amino acid.[50–53] Some recently characterized examples include subtilosin A, subtilosin A1,[49,51] thuricin CD (composed of two peptides, thuricin α and thuricin β),[52] and thuricin H.[53] In the biosynthesis of subtilosin A, AlbA is a radical SAM enzyme with two [4Fe-4S] clusters. The first cluster undergoes reductive cleavage of SAM to produce 5′-dAdo• [**16** → **18** conversion (Figure 4)], which then abstracts a hydrogen from the α-position of the amino acid, where the thioether bond will be formed [**23** → **23a** conversion (Figure 6)]. The role of the auxiliary [4Fe-4S] cluster in AlbA catalysis is not yet well-defined, but two mechanisms have been proposed (Figure 6). In the first model [pathway I (Figure 6)],[49] SAM binds to the unique iron site of the first [4Fe-4S] cluster, while the sulfur group from the peptide substrate coordinates to one of the irons of the auxiliary [4Fe-4S] cluster [**23b** (Figure 6)]. The substrate-based radical reacts with the cysteine sulfur to form the thioether bond [**23a** → **23b** conversion (Figure 6)]. At the same time, one electron is transferred from the substrate to reduce the auxiliary [4Fe-4S] cluster. In this model, the auxiliary [4Fe-4S] cluster serves as an electron acceptor. After the product is released, the reduced auxiliary cluster relays the electron back to the first [4Fe-4S] cluster to initiate another catalytic cycle.

In the other model [pathway II (Figure 6)], substrate-based radical **23a** is oxidized by the auxiliary $[4Fe\text{-}4S]^{2+}$ cluster. The intermediate is then trapped by the sulfur from a cysteine residue in the substrate to form a thioether [**23c** → **24** conversion (Figure 6)]. In this pathway, the auxiliary [4Fe-4S] cluster is also key to the redox chemistry required for thioether formation, while a direct coordination between the substrate and the auxiliary

[4Fe-4S] cluster is not necessary.[54] Additional studies are required to differentiate between these two models.

In the biosynthesis of penicillin, isopenicillin *N*-synthase (IPNS) is responsible for installing β-lactam and thiazolidine rings through an aerobic radical type of sulfur insertion mechanism (Figure 7). IPNS is a mononuclear non-heme iron enzyme, which catalyzes a four-electron oxidation of a tripeptide δ-(L-α-aminoadipoyl)-L-cysteinyl-D-valine (LLD-ACV, **25**) to isopenicillin *N* **26** (Figure 7).[55,56] After binding and activation of oxygen by the Fe^{II} center, the Fe^{III}–superoxo intermediate oxidizes the cysteine sulfur to generate a thiolaldehyde **25a**, which is attacked by the valine amide to form the β-lactam ring. Heterolytic cleavage of the O–O bond of the hydroperoxo intermediate generates Fe^{IV}═O species **25b**, which abstracts a hydrogen atom from the $C_{Val,\beta}$ position, resulting in a valinyl radical **25c**. Subsequently, the thiazolidine ring is formed by combining a valinyl radical and a thiol radical to produce the final product, isopenicillin *N* **26**.[57]

There is currently growing interest in the biosynthesis of sulfur-containing natural products. The examples mentioned above represent some of the general strategies. Many of the recently discovered biosynthetic pathways for sulfur-containing natural products have not yet been biochemically characterized. In the next section, we summarize the sulfur transfer strategy in ergothioneine and ovothiol biosynthesis in which sulfur is incorporated through a combination of a mononuclear non-heme iron enzyme-catalyzed oxidative C–S bond formation reaction and a PLP enzyme-mediated C–S lyase reaction. This sulfur transfer strategy differs from all other examples discussed in previous sections (Figures 1–7).

BIOSYNTHESIS OF ERGOTHIONEINE AND OVOTHIOL

Early Ergothioneine Biosynthetic Studies Using Isotopically Labeled Precursors

Ergothioneine **32** and ovothiol **36a**–**c** are histidine derivatives with sulfur substitutions at the ε-and δ-carbons of the histidine imidazole side chain, respectively. Ergothioneine [**32** (Figure 8A)] was isolated from ergot by Tanret in 1909.[58] The biosynthetic community began the search for the ergothioneine biosynthetic details as early as the 1950s. At that time, ergothioneine had been isolated from various microorganisms.[59–61] Feeding studies of ergothioneine-producing strains led to the structural characterization of some of the key intermediates. Culturing ergothioneine-producing strain *Claviceps purpurea* with [2-^{14}C]acetate showed that L-His and ergothioneine have similar labeling distribution patterns, suggesting that L-His is an ergothioneine biosynthetic precursor.[62] When [^{14}C]His was fed to *Neurospora crassa*, it was efficiently incorporated into ergothioneine, whereas [^{14}C]-thiohistidine was not.[63] On the basis of these results, it was suggested that hercynine **28** is most likely an intermediate in ergothioneine biosynthesis. The source of sulfur was also examined, and feeding studies indicated that thiosulfate and some sulfur-containing amino acids (e.g., cysteine and cystine) were the sulfur sources for ergothioneine. Using [^{14}C]methyl-labeled methionine resulted in ergothioneine with ^{14}C-labeled methyl groups, suggesting that methionine is the methyl source for ergothioneine. Feeding experiments in *C. purpurea* led to similar conclusions.[63–65]

These early feeding studies suggested that ergothioneine biosynthesis most likely starts with the methylation of the L-His amino group to produce hercynine **28** (Figure 8A).[66] This conclusion was further substantiated by using *N. crassa* cell extract, which catalyzes the conversion of L-His to hercynine using SAM as the methyl source.[67,68] When [^{14}C]hercynine and L-Cys were incubated with *N. crassa* cell extract, the production of ergothioneine was observed. Interestingly, in the presence of 200 μM hydroxylamine, *S*-(β-amino-β-carboxyethyl)ergothioneine sulfoxide **31** accumulated. In addition, adding *S*-(β-amino-β-carboxyethyl)ergothioneine sulfoxide **31** to the *N. crassa* cell extract resulted in ergothioneine production.[69] Results from these studies suggested that sulfoxide **31** might be another ergothioneine biosynthetic intermediate (Figure 8A).

The exact enzymes responsible for these transformations in ergothioneine biosynthesis were not identified at that time. However, it was discovered that supplementing the *N. crassa* cell extract with Fe^{2+} and pyridoxamine phosphate (PLP) significantly improved the ergothioneine production yield. The identities of these enzymes were uncovered recently,[70] and their biochemical properties correspond to the observations in the study of *N. crassa* cell extract.

Ovothiol Biosynthetic Studies Using Cell Extracts

Ovothiol A **36a** is another thiohistidine isolated from eggs and ovaries of marine invertebrates[71] and trypanosomatids (Figure 8B).[72,73] Similar to the ergothioneine studies, the initial characterizations of ovothiol A biosynthetic studies were conducted using the cell extracts from ovothiol-producing organisms. Using *Crithidia fasciculate*, an ovothiol-producing organism, Steenkamp et al. demonstrated that ovothiol is derived from L-His and L-Cys and that the sulfur transfer occurs prior to methylation.[74] Using partially purified proteins from *Cr. fasciculate*, Steenkamp and co-workers further demonstrated that ovothiol A biosynthesis also involves an iron enzyme-catalyzed oxidative coupling reaction and a PLP-catalyzed C–S lyase reaction.[75] Thus far, only the identity of the non-heme iron enzyme is known.[76]

Ergothioneine and Ovothiol Biosynthetic Pathways

Recently, Seebeck and co-workers discovered the ergothioneine biosynthetic gene cluster using a comparative genomic approach (Figure 8A).[77] In one of the ergothioneine-producing organisms, *Mycobacterium aviu*, there are 78 annotated methyltransferases, and among these genes, 29 of them have homologues in *N. crassa*, another ergothioneine-producing species. Eliminating homologues in ergothioneine nonproducing species narrows the list to 10 candidate methyltransferases. Interestingly, one of them is located next to a PLP-containing enzyme in the context of a five-gene cluster, designated *egtABCDE* (EgtA–EgtE genes). The recombinant EgtD indeed catalyzes the methylation of L-His **27** to hercynine **28**, and the methylation is processive (Figure 8A), resulting in hercynine **28** with only small amounts of mono- or dimethylhistidine products. This processivity is attributed to the fact that EgtD binds to dimethyl-histidine 70-fold more tightly than to histidine.[78]

Feeding study results discussed previously implied that an Fe-dependent enzyme is responsible for oxidative C–S bond formation. Indeed, EgtB in the gene cluster reported by

Seebeck is a non-heme iron enzyme. In addition, the presence of γ-glutamyl-cysteine ligase (EgtA) in the mycobacterium ergo-thioneine biosynthetic gene cluster suggests that γ-glutamyl-cysteine **29** is the sulfur source.[77] As expected, EgtB catalyzes the oxidative coupling between hercynine and γ-glutamyl-cysteine to form a sulfoxide **30**. Then, the glutamate group is removed by a glutamine amidotransamidase homologue (EgtC). The last step of ergothioneine biosynthesis is catalyzed by a PLP-dependent C–S lyase (EgtE), whose activity has also been demonstrated *in vitro*.[79,80] Recently, OvoA, an EgtB homologue, was identified from one of the ovothiol A producers, *Erwinia tasmaniensis*.[76] Recombinant OvoA catalyzes the oxidative coupling between L-His **27** and cysteine to a sulfoxide **33** *in vitro* (Figure 8B). However, the proposed C–S lyase and methyltransferase in ovothiol biosynthesis remain to be identified.

Biochemical Information about Ergothioneine and Ovothiol Biosynthesis

In ergothioneine and ovothiol biosyntheses, the trans-sulfuration method differs from those discussed previously (Figures 1–7). A combination of a non-heme iron enzyme-catalyzed oxidative C–S bond formation (EgtB, OvoA catalysis) and a reductive C–S lyase represents one of the most efficient sulfur transfer strategies in natural product biosyntheses. After the discovery of the mycobacterial EgtB gene, the functions of its homologues in fungi (*N. crassa*,[81] *Aspergillus fumigates*,[82] and the fission yeast, *Schizosaccharomyces pombe*[83]) have also been examined by genetic studies. A systematic analysis of all completed genomes in the NCBI database indicated that ergothioneine biosynthetic genes are widely distributed in actinobacteria,[84] while EgtB and EgtD were found across proteobacterial and cyanobacterial species.[85]

EgtB and OvoA both mediate sulfoxide formation; however, they differ in their substrate selectivity and C–S bond formation regioselectivity (panel A vs panel B of Figure 8). In ergothioneine biosynthesis, EgtB makes use of hercynine and γ-glutamyl-cysteine as the substrates and the C–S bond is formed at the ε-position (Figure 8A). OvoA, on the other hand, uses L-His and L-Cys as the substrates, resulting in the C–S bond being formed at the δ-position (Figure 8B). Interestingly, with hercynine **28** as the substrate, OvoA catalyzes the oxidative coupling between hercynine and L-Cys to hercynyl-cysteine sulfoxide [**31** (Figure 8C)].[86,87] OvoA also mediates the oxidation of cysteine to cysteine sulfinic acid **34** (Figure 8C), an activity solely reported in cysteine dioxygenase (CDO).[88] On the basis of the EgtB and OvoA biochemical information and guided by sequence similarity network analysis results, we identified and characterized the Egt1 gene from fungal *N. crassa* biochemically *in vitro*. The fungal Egt1 preferentially catalyzes the oxidative coupling between hercynine **28** and L-Cys to give hercyl-cysteine sulfoxide **31** (Figure 8A).[70] These studies led to the elucidation of two aerobic ergothioneine biosynthetic pathways: the mycobacterial pathway[77] [EgtA–EgtE (Figure 8A)] and the fungal *N. crassa* pathway[70] [Egt1 and Egt2 (Figure 8A)].

The discoveries of these aerobic ergothioneine biosynthetic pathways are in line with the function of ergothioneine as a cellular antioxidant. Seebeck and co-workers analyzed the genomes of a green sulfur bacterium *Chlorobium limicola* DSM 245 and identified Clim_1148 (EanA) as an EgtD homologue.[89] *Ch. limicola* grows in illuminated anoxic

waters and conducts anaerobic photosynthesis using sulfides as the electron donor for carbon dioxide fixation. The recombinant EanA can catalyze the methylation of L-His **27** to hercynine **28**. Analysis of the EanA gene neighborhood revealed a putative rhodanese-like sulfur transferase (EanB, Clim_1149). This pair of enzymes was found in at least 20 genomes from predominantly anaerobic bacteria and archaea. In the presence of cysteine desulfurase IscS, EanB can mediate the transfer of sulfur from cysteine to hercynine **28** to yield ergothioneine (Figure 8D). This surprising discovery contradicts the general hypothesis of having ergothioneine as an antioxidant, which removes reactive oxygen species (ROS) or reactive nitrogen species (RNS) generated under aerobic conditions.[90] The presence of ergothioneine in anaerobic organisms raised the question of its biological functions. In addition, the trans-sulfuration catalyzed by EanB is intriguing because this transformation differs from other rhodanase-catalyzed sulfur transfer reactions (Figure 3). This discovery suggests that at least three different ergothioneine biosynthetic pathways exist in nature: two aerobic and one anaerobic (Figure 8A,D).[91]

Mechanistic Characterization of Oxidative C–S Bond Formation in Ergothioneine and Ovothiol Biosyntheses

The crystal structure of *Mycobacterium thermoresistible* EgtB has been reported.[92] It has an N-terminal DinB-like four-helix bundle (residues 7–150) and a C-terminal C-type lectin fold. The EgtB structure contains few secondary structural elements and is rich in loops stabilized by buried ionic interactions (Figure 9A). The enzyme active site is in a 15 Å deep and 10 Å wide tunnel, and at the bottom of the tunnel, the catalytic iron is coordinated by three histidine residues (H51, H134, and H138). The Fe^{2+} center is also coordinated to three water ligands. When the Fe^{2+} center was replaced with Mn^{2+}, the structure of the EgtB·dimethylhis-tidine·γ-glutamyl-cysteine tertiary complex was obtained (Figure 9B). Dimethylhistidine (DMH) coordinates to the Mn^{2+} center using its imidazole side chain, while γ-glutamyl-cysteine coordinates to the metallocenter using its side chain sulfur. The sixth ligand is a water molecule, which is most likely the site for oxygen binding and activation. In this structure, the water ligand is hydrogen-bonded to the hydroxyl group of an active site tyrosine residue (Y377). Upon mutation of Y377 to F377 in EgtB, the dominant activity of this mutant is the cysteine dioxygenase activity [k_{cat} of 1.2 s^{-1} (Figure 8E)], instead of oxidative C–S bond formation in wild-type EgtB. This activity is at a level comparable to that of native CDO activity (k_{cat} of 1.8 s^{-1}).[93,94] This discovery suggested that Y377 might serve as a general acid–base or be part of the redox chemistries in EgtB catalysis.

The kinetic parameters (k_{cat} and K_m values for hercynine and γ-glutamyl-cysteine) for EgtB Y377F are very similar to those of wild-type EgtB.[93] As in the case of wild-type OvoA catalysis, the γ-glutamyl-cysteine dioxygenase activity depends on the presence of hercynine **28**. In the absence of hercynine **28**, γ-glutamyl-cysteine is oxidized to γ-glutamyl-cystine at a rate orders of magnitude lower than the γ-glutamyl-cysteine sulfinic acid or sulfoxide formation rates. Cysteine sulfinic acid formation and sulfoxide formation are possibly two pathways branching out from a common intermediate in both EgtB and OvoA catalysis (Figure 8).[93,95]

These two reactions have also been characterized by studies measuring the kinetic isotope effect (KIE). Using [ε-^{2}H]-hercynine **28** as the substrate, no primary KIEs were observed. The solvent KIEs on wild-type EgtB and the EgtB Y377F mutant were measured for both the γ-glutamyl-cysteine dioxygenase activity and the sulfoxide synthase activity. The solvent KIEs for wild-type EgtB sulfoxide synthase and Y377F mutant γ-glutamyl-cysteine dioxygenase activity were 1.2 ± 0.2 and 0.9 ± 0.1, respectively. For the sulfoxide synthase activity of the EgtB Y377F mutant, the determined solvent KIE is 1.9 ± 0.1.[93] The chemistries involved in the ergothioneine and ovothiol biosynthetic pathways are very similar (Figure 8) despite the differences in substrate selectivity and product regioselectivity between EgtB/Egt1 and OvoA.[70,76,77,86,95] In addition, cysteine dioxygenase activity was discovered in OvoA (Figure 8C).[95] Although wild-type EgtB does not show γ-glutamyl-cysteine dioxygenase activity, the dominant reaction in the EgtB Y377F mutant is γ-glutamyl-cysteine dioxygenase activity (Figure 8E).[93] The discovery of sulfur oxidation[88,96,97] in EgtB and OvoA adds another level of complexity to their mechanistic investigations. Both EgtB catalysis and OvoA catalysis are four-electron oxidations, in which molecular oxygen is fully reduced to water. In this process, oxidative C–S bond formation and formation of sulfoxide each provide two electrons. In EgtB and OvoA catalysis, it has yet to be determined whether C–S bond formation or sulfur oxidation occurs first. Several mechanistic options have been proposed for EgtB and OvoA reactions.[76,95]

Using EgtB catalysis as the example, the proposed mechanistic models and roles of Y377 are summarized (Figure 10). The EgtB mononuclear iron center has three histidine ligands and three exchangeable water ligands. In pathway I (Figure 10), the binding of substrates, γ-glutamyl-cysteine and hercynine, replaces two exchangeable H_2O ligands. The remaining ligand site is for oxygen binding and activation to produce Fe^{III}–superoxo species, which reacts with the thiolate to form a γ-glutamyl-cysteine sulfenic acid and an Fe^{IV}═O species [**38b** (Figure 10)]. After formation of the Fe^{IV}═O species, both two-electron chemistry and one-electron chemistries have been proposed for the subsequent steps [pathways IA–IC (Figure 10)].[76,98–100] The Fe^{IV}═O species may abstract a hydrogen atom from the histidine imidazole ring δ-carbon to produce an imidazole-based radical [**38c**, pathway IA (Figure 10)]. Subsequently, the C–S bond forms by combining the thiol radical with the imidazole radical (**38c** → **30**). Alternatively, one electron transfer from the imidazole ring to the Fe^{IV}═O species results in an imidazole cation radical [**38d**, pathway IB (Figure 10)]. After the C–S bond is formed (**38d** → **38e**), Y377 is proposed to function as a base to deprotonate **38e** to finish the catalytic cycle (**38e** → **30**). It has also been suggested that direct nucleophilic attack by the imidazole on the sulfenic acid functional group leads to C–S bond formation [**38b** → **38e**, pathway IC (Figure 10)]. Subsequent deprotonation of the imidazole ring in **38e** by a base, potentially Y377, results in coupling product **30**.

Recently, the cysteine dioxygenase activity and the sulfoxide formation activity of EgtB have been examined through quantum mechanics/molecular mechanics (QM/MM)-based calculations (energy diagram in Figure 10B) using the *M. thermoresistibile* EgtB structure as a starting point.[98] In the mechanistic model reported by Visser and co-workers, when oxygen binds to the iron center, the first intermediate is an Fe^{III}–superoxo intermediate [**38f**, pathway II (Figure 10)]. In the subsequent step, the hydrogen bond network between Y377

and the active site water allows a proton-coupled electron transfer process to occur to produce Fe^{III}–hydroperoxo species **38g** along with a tyrosyl radical. Then, a nucleophilic or radical attack of the cysteine sulfur atom on the imidazole side chain of hercynine links the two substrates together through a thioether linkage (**38g** → **38h**). Simultaneously with C–S bond formation, the hydrogen atom of hydroperoxo species is relayed back to the Y377-based radical to regenerate tyrosine and at the same time leads to an Fe^{II}–superoxo intermediate **38h**. In the next step, the Fe^{II}–superoxo intermediate abstracts a hydrogen atom from the imidazole ring to regenerate the aromaticity and produces the Fe^{II}–hydroperoxo intermediate [**38i** (Figure 10)]. In this pathway, the C–S bond formation step, specifically, the formation of intermediate **38h** is the rate-limiting step with an energy barrier of ~14.2 kcal/mol (Figure 10B). For **38h** → **38i** conversion, the energy barrier is ~4.4 kcal/mol and the transition from **38i** to the product complex is energetically favorable (Figure 10B). The results from QM/MM-based mechanistic studies suggested that Y377 is involved in EgtB catalysis through a proton-coupled electron transfer process to reduce superoxo intermediate **38f** to a hydroperoxo intermediate **38g**. This model differs from the model proposed by Seebeck originally, in which the Y377 serves as a Lewis acid to provide a proton to peroxo species to produce a hydroperoxo intermediate.[92] In addition, Visser and co-workers also proposed that the reduction of Fe^{III}–superoxo intermediate **38f** by a proton-coupled electron transfer process from Y337 plays the key role in suppressing thiol dioxygenase activity [**38b** → **37** (Figure 10A)].

Starting from the same *M. thermoresistibile* EgtB structure, Wei et al. also examined the EgtB catalytic mechanism using density functional theory.[99] In this work, it is proposed that the first half of EgtB catalysis undergoes the sulfur oxidation to generate a sulfenic acid intermediate along with Fe^{IV}═O species **38b**. Wei et al. proposed that the deprotonation of **38e** is the rate-limiting step (pathway IB in Figure 10A), and a KIE as high as 5.7 was predicted. Thus far, KIEs measured from at least two reports were all close to unity, far from the predicted value of 5.7.[87,100]

There is currently no crystal structure for OvoA; therefore, we generated an OvoA structure model using I-TASSER.[101] In this model, Y417 in OvoA is likely the EgtB Y377 counterpart.[100] Wild-type OvoA has ~10% cysteine dioxygenase activity (Figure 8B). Replacing Y417 with a tyrosine analogue, 2-amino-3-[4-hydroxy-3-(methylthio)phenyl] propanoic acid [MtTyr, **39** (Figure 11A)], a mimic of the tyrosine–cysteine cross-link in cysteine dioxygenase,[102–104] resulted in 30% cysteine dioxygenase activity (Figure 11A,B). In addition, for the OvoA Y417MtTyr variant, the amount of cysteine sulfinic acid further increases from 30% in H_2O buffer to approximately 50% in D_2O buffer. These results demonstrated that the two activities in OvoA catalysis can be modulated by replacing the active site tyrosine using a tyrosine analogue.[100] Further systematic characterization using tyrosine analogues could provide mechanistic insights related to these novel transformations. Thus far, no mechanistic information for the anaerobic ergothioneine biosynthetic pathway is available (Figure 8D).[89]

Mechanistic Studies of the C–S Lyase in Ergothioneine Biosynthesis

In ergothioneine and ovothiol biosynthesis, aside from the non-heme iron-dependent enzyme-catalyzed oxidative C–S bond formation (EgtB, Egt1, and OvoA catalysis), the other novel transformation is the EgtE/Egt2-catalyzed C–S lyase reaction. Most of the reported C–S lyases use thioethers as the substrates.[105] The C–S lyase (EgtE/Egt2) in ergothioneine biosynthesis, however, is among the few lyases using sulfoxide substrates.[79,106] Through a combination of biochemical and structural approaches, we have characterized how the reduction process is coupled with the C–S lyase reaction. Recombinant EgtE makes use of both thioether **40** and sulfoxide **31** as its substrate; pyruvate **41** and ammonia were produced as the side products (Figure 12A).[79] Using thiol ether **40** as the substrate, ergothioneine was produced in a reductant-independent manner. When hercyl-cysteine sulfoxide **31** was used as the substrate in the absence of a reductant, ergothioneine **32** and ergothioneine-2-sulfinic acid **42b** were isolated in a 1:1 ratio (Figure 12B). A plausible explanation for this result is that ergothioneine sulfenic acid **42** is the product of EgtE/Egt2 catalysis (Figure 12B). After intermediate **42** is released from the EgtE/Egt2 active site, a disproportionation reaction between two molecules of ergo-thioneine sulfenic acid **42** leads to the formation of a thio-sulfinic acid **42a**, which is hydrolyzed to ergothioneine **32** and ergothioneine-2-sulfinic acid **42b** (Figure 12B). The spontaneous decomposition of ergothioneine sulfinic acid **42b** produces hercynine and SO_2. In the presence of DTT, ergothioneine sulfenic acid **42** is reduced to ergothioneine (Figure 12A). The sulfenic acid intermediate **42** has also been trapped using 1,3-cyclohexanedione, and the adduct was isolated and characterized.[80]

Recently, we have successfully determined the crystal structure of Egt2 (the *N. crossa* ergothioneine C–S lyase).[80] In its native structure, PLP is covalently linked to Egt2 protein through a Schiff base with K247. The pyridine ring of PLP interacts with the aromatic ring of Y134 via π–π stacking interactions. The Egt2 Y134F mutant is much less active than wild-type Egt2, while this Egt2 Y134F mutant still maintains some enzymatic activity [k_{cat}/K_m of (4.8 ± 0.1) × 10^{-3} μM^{-1} s^{-1} at pH 7.0, which is ~11.5-fold lower than that of wild-type Egt2]. The low activity of the Egt2 Y134F mutant allowed us to capture several intermediates in Egt2 catalysis (Figure 13). In one of the monomers, the active site electron density is consistent with the assignment of the Egt2 Y134F·substrate **31** binary complex prior to external aldimine intermediate formation (Figure 13B). When the crystals were transferred to a cryo buffer (pH 8.0), the electron density of the active site suggests that the chemical reaction has occurred, and a sulfenic acid intermediate in Egt2 catalysis was trapped (Figure 13C). In addition to the sulfenic acid intermediate, the positive density next to the PLP C4′ position in one of the EgtE monomers is consistent with an aminoacrylate geminal diamine intermediate (Figure 13D).

On the basis of these biochemical and structural studies, a mechanistic model was proposed (Figure 13E). Similar to other PLP-containing enzymes, the first step is the formation of external aldimine intermediate **31a** between the PLP cofactor and sulfoxide substrate **31**. After deprotonation of the Cys α-carbon to generate a quinonoid intermediate **31b**, subsequent C–S bond cleavage produces ergothioneine sulfenic acid **42** and the PLP-based aminoacrylate intermediate, which decomposes to pyruvate **41** and ammonia. Egt2 structural

analysis reveals a C156 residue located adjacent to the active site exit, implying that C156 might trap ergothioneine sulfenic acid **42** to produce a disulfide intermediate. This intermediate is then reduced to ergothioneine and regenerates C156 for the next cycle [pathway I (Figure 13E)]. Alternatively, ergothioneine sulfenic acid **42** formed might be released to the solution directly, which is then reduced to ergothioneine by either a small molecular reductant (e.g., glutathione) or a thiol reduction system [e.g., the thioredoxin/thioredoxin reductase pair, pathway II (Figure 13E)].

Ergothioneine Biological Functions

In humans, ergo-thioneine accumulates in many tissues with concentrations ranging from 100 μM to 2 mM, with the highest concentrations being in erythrocytes, bone marrow, liver, kidney, seminal fluid, and the lens and cornea of eyes,[107–110] through an ergothioneine-specific transporter, OCTN1.[110]

The concentrations of ergothioneine in various tissues are correlated with the abundance of *OCTN1* mRNA.[111–113] In addition, when *OCTN1* was deleted, ergothioneine accumulation is abolished, which suggests that OCTN1-mediated uptake is probably the sole ergothioneine uptake mechanism in animals.[114,115] Ergothioneine has been suggested to play a role complementary to that of glutathione *in vivo*.[90] The exact biological target of ergothioneine remains to be identified. Ergothioneine's reduction potential ($E_0{}' = -0.06$ V[3,116,117]) is significantly higher than that of glutathione ($E_0{}' = -0.25$ V[118]). It has been suggested that the primary role of ergothioneine is as an antioxidant to eradicate reactive oxygen species (ROS) and reactive nitrogen species (RNS),[90] including $^{\bullet}OH$, peroxyl radicals, peroxynitrite ($ONOO^-$), nitrosoperoxycarbonate ($ONOOCO_2^-$), and carbonate radical. Several human diseases have been suggested to be related to ergothioneine, including rheumatoid arthritis,[119,120] Crohn's disease,[121,122] neurodege-nerative diseases,[123–126] cardiovascular disorders,[127] and diabetes.[128] Ergothioneine can pass through the blood–brain barrier[123–125] and might serve as a protection mechanism against neurodegenerative diseases. Overstimulation of *N*-methyl-D-aspartate (NMDA) leads to neuronal cell death due to an increased level of production of free radicals.[129] Intravitreal injection of NMDA in rats leads to a significant loss of retinal neurons. However, the NMDA excitotoxicity was relieved by intraperitoneal injection of ergothioneine.[126] Ergothioneine treatment decreases the level of expression of adhesion molecules VACM-1, ICAM-1, and E-selectin. As a result, it inhibits the binding of monocytes to the endothelium,[130] which might be the reason explaining ergothioneine's protective effects against cardiovascular disorders.[127]

Because of the wide distribution of ergothioneine in both aerobic and anaerobic systems, it is tempting to assume that ergothioneine may have biological roles besides being a biological antioxidant.[89,91] Recently, Zhao et al. reported the biochemical characterization of lincomycin A biosynthesis, in which ergothioneine plays a key role (Figure 14).[131] Lincomycin **49** is an antibiotic produced from *Streptomyces lincolnensis*. It has an *N*-methyl-4-propyl-L-Pro (PPL) moiety and an unusual eight-carbon sugar (lincosamide) decorated with a C-1 position methylthiol group. In the licomycin A (**49**) biosynthetic gene cluster, there is a DinB-2-like domain-containing protein, LmbV. DinB-2 domain-containing

proteins make up a large superfamily with more than 10000 members, which are involved in the transformations using small molecular thiols.[132] LmbV was proposed to mediate the incorporation of the thiol group at the lincosamide C-1 position. In the Δ*lmbV* mutant, as anticipated, no lincomycin A was produced. Surprisingly, an ergothioneine S-conjugate **46** was isolated. To further characterize the function of LmbV, Zhao et al. overexpressed and isolated a LmbV homologue (CcbV, 57% identical to LmbV) because LmbV overexpression was challenging. When ergothioneine S-conjugate **46** and MSH were supplied as the CcbV substrates, MSH S-conjugate **47** was observed along with the formation of ergothioneine as the side product.[131] This was the first discovery of ergothioneine being involved in sugar activation.

Sequence analysis suggests that LmbT is a glycosyltransferase. *In vitro* characterization demonstrated that LmbT mediates the equilibrium between GDP-lincosamide and the lincosamide–ergothioneine conjugate [**44** → **45** (Figure 14)]. The LmbT-catalyzed reaction exhibited an equilibrium constant K_{eq} of 1.94, and the reaction slightly favors GDP-lincosamide **44**.

Subsequent genetic and biochemical characterizations suggested that LmbC, LmbD, and LmbN work together to incorporate the PPL moiety into the lincosamide–ergothioneine conjugate to produce **46**. LmbC encodes an adenylation protein, which activates PPL using ATP and transfers PPL onto the peptidyl carrier protein (PCP) domain of LmbN protein. LmbD then catalyzes the condensation between the activated PPL and EGT S-conjugate **45** to yield **46**. In the lincomycin-producing organism, *S. lincolnensis*, LmbE is an amidase homologue. As predicted, a MSH-associated lincomycin analogue **47** accumulated in the Δ*lmbE* mutant strain. The recombinant LmbE rapidly converts **47** to 1-*O*-(2-*N*-acetyl)-glucosamine-D-*myo*-inositol-3-phosphate (GlcNAc-Ins-3-P) and **48**. Thus far, most of the critical steps in licomycin A **49** biosynthesis have been established. This biosynthetic process involves two small molecular thiols, mycothiol (MSH) and ergothioneine (EGT).

Over the years, it has been suggested that small molecular thiols are involved in providing protection against oxidative stress or employed as tools to detoxify electrophilic toxins. The discovery of the key roles played by ergothioneine in lincomycin A biosynthesis is the first example of its involvement in a natural product biosynthetic pathway. Several biosynthetic pathways have been suggested to involve MSH S-conjugates. Given the presence of ergothioneine across biological systems, it is likely that many more roles of ergothioneine may be discovered in the future.[133,134] *S*-Alk(en)yl-L-Cys sulfoxides have been discovered as metabolites in many plants, and some of them play important biological roles, e.g., suppression of hypercholesterolemia,[135] stimulation of insulin secretion,[136] or priming neutrophils for respiratory burst.[137] In addition to an examination of the roles of ergothioneine and ovothiol, it may also be beneficial to characterize the biological function of ergothioneine and ovothiol biosynthetic intermediates (Figure 8).

In summary, ergothioneine and ovothiol biosynthetic studies not only provide an excellent system for characterizing new trans-sulfuration strategies in nature but also offer ample opportunities for future investigations of the biological functions of small molecular thiols.

Acknowledgments

Funding

This work is supported in part by grants from the National Institutes of Health (R01 GM093903) and the National Science Foundation (CHE-1309148) to P.L. and a grant from National Natural Science Foundation of China (31670030) to C.Z. L.C. and C.Z. are supported by fellowships from the China Scholarship Council. N.N. is supported by a Warren-McLoed fellowship from the Boston University Marine Program.

References

1. Kessler D. Enzymatic activation of sulfur for incorporation into biomolecules in prokaryotes. FEMS Microbiol Rev. 2006; 30:825–840. [PubMed: 17064282]
2. Hand CE, Honek JF. Biological chemistry of naturally occurring thiols of microbial and marine origin. J Nat Prod. 2005; 68:293–308. [PubMed: 15730267]
3. Fahey RC. Novel thiols of prokaryotes. Annu Rev Microbiol. 2001; 55:333–356. [PubMed: 11544359]
4. Mueller EG. Trafficking in persulfides: delivering sulfur in biosynthetic pathways. Nat Chem Biol. 2006; 2:185–194. [PubMed: 16547481]
5. Shigi N. Biosynthesis and functions of sulfur modifications in tRNA. Front Genet. 2014; 5:67. [PubMed: 24765101]
6. Fontecave M, Atta M, Mulliez E. *S*-adenosylme-thionine: nothing goes to waste. Trends Biochem Sci. 2004; 29:243–249. [PubMed: 15130560]
7. Struck AW, Thompson ML, Wong LS, Micklefield J. *S*-adenosyl-methionine-dependent methyltransferases: highly versatile enzymes in biocatalysis, biosynthesis and other biotechnological applications. ChemBioChem. 2012; 13:2642–2655. [PubMed: 23180741]
8. Beld J, Sonnenschein EC, Vickery CR, Noel JP, Burkart MD. The phosphopantetheinyl transferases: catalysis of a post-translational modification crucial for life. Nat Prod Rep. 2014; 31:61–108. [PubMed: 24292120]
9. Begley TP, Xi J, Kinsland C, Taylor S, McLafferty F. The enzymology of sulfur activation during thiamin and biotin biosynthesis. Curr Opin Chem Biol. 1999; 3:623–629. [PubMed: 10508664]
10. Jurgenson CT, Begley TP, Ealick SE. The structural and biochemical foundations of thiamin biosynthesis. Annu Rev Biochem. 2009; 78:569–603. [PubMed: 19348578]
11. Berkovitch F, Nicolet Y, Wan JT, Jarrett JT, Drennan CL. Crystal structure of biotin synthase, an *S*-adenosylmethionine-dependent radical enzyme. Science. 2004; 303:76–79. [PubMed: 14704425]
12. Ugulava NB, Frederick KK, Jarrett JT. Control of adenosylmethionine-dependent radical generation in biotin synthase: a kinetic and thermodynamic analysis of substrate binding to active and inactive forms of BioB. Biochemistry. 2003; 42:2708–2719. [PubMed: 12614166]
13. Ugulava NB, Gibney BR, Jarrett JT. Biotin synthase contains two distinct iron-sulfur cluster binding sites: chemical and spectroelectrochemical analysis of iron-sulfur cluster interconversions. Biochemistry. 2001; 40:8343–8351. [PubMed: 11444981]
14. Ugulava NB, Sacanell CJ, Jarrett JT. Spectroscopic changes during a single turnover of biotin synthase: destruction of a [2Fe-2S] cluster accompanies sulfur insertion. Biochemistry. 2001; 40:8352–8358. [PubMed: 11444982]
15. Booker SJ, Cicchillo RM, Grove TL. Self-sacrifice in radical *S*-adenosylmethionine proteins. Curr Opin Chem Biol. 2007; 11:543–552. [PubMed: 17936058]
16. Schwarz G, Mendel RR, Ribbe MW. Molybdenum cofactors, enzymes and pathways. Nature. 2009; 460:839–847. [PubMed: 19675644]
17. Graham DE, White RH. Elucidation of methanogenic coenzyme biosyntheses: from spectroscopy to genomics. Nat Prod Rep. 2002; 19:133–147. [PubMed: 12013276]
18. Fontecave M, Ollagnier-de-Choudens S, Mulliez E. Biological radical sulfur insertion reactions. Chem Rev. 2003; 103:2149–2166. [PubMed: 12797827]

19. Graham DE, Xu HM, White RH. Identification of coenzyme M biosynthetic phosphosulfolactate synthase - A new family of sulfonate-biosynthesizing enzymes. J Biol Chem. 2002; 277:13421–13429. [PubMed: 11830598]
20. Dunbar KL, Scharf DH, Litomska A, Hertweck C. Enzymatic carbon-sulfur bond formation in natural product biosynthesis. Chem Rev. 2017; 117:5521–5577. [PubMed: 28418240]
21. Repka LM, Chekan JR, Nair SK, van der Donk WA. Mechanistic understanding of lanthipeptide biosynthetic enzymes. Chem Rev. 2017; 117:5457–5520. [PubMed: 28135077]
22. Waldman AJ, Ng TL, Wang P, Balskus EP. Heteroatom-heteroatom bond formation in natural product biosynthesis. Chem Rev. 2017; 117:5784–5863. [PubMed: 28375000]
23. Gilbert JA, Jansson JK, Knight R. The Earth Microbiome Project: successes and aspirations. BMC Biol. 2014; 12:69. [PubMed: 25184604]
24. Li B, Yu JPJ, Brunzelle JS, Moll GN, van der Donk WA, Nair SK. Structure and mechanism of the lantibiotic cyclase involved in nisin biosynthesis. Science. 2006; 311:1464–1467. [PubMed: 16527981]
25. Willey JM, van der Donk WA. Lantibiotics: peptides of diverse structure and function. Annu Rev Microbiol. 2007; 61:477–501. [PubMed: 17506681]
26. Davis C, Carberry S, Schrettl M, Singh I, Stephens JC, Barry SM, Kavanagh K, Challis GL, Brougham D, Doyle S. The role of glutathione *S*-transferase GliG in gliotoxin biosynthesis in *Aspergillus fumigatus*. Chem Biol. 2011; 18:542–552. [PubMed: 21513890]
27. Scharf DH, Chankhamjon P, Scherlach K, Heinekamp T, Willing K, Brakhage AA, Hertweck C. Epidithiodike-topiperazine biosynthesis: a four-enzyme cascade converts glutathione conjugates into transannular disulfide bridges. Angew Chem, Int Ed. 2013; 52:11092–11095.
28. Haeggstrom JZ, Funk CD. Lipoxygenase and leukotriene pathways: biochemistry, biology, and roles in disease. Chem Rev. 2011; 111:5866–5898. [PubMed: 21936577]
29. Hammerstrom S, Samuelsson B. Detection of leukotriene-A4 as an intermediate in the biosynthesis of leukotriene-C4 and leukotriene-D4. FEBS Lett. 1980; 122:83–86. [PubMed: 6260529]
30. Hansen CH, Du L, Naur P, Olsen CE, Axelsen KB, Hick AJ, Pickett JA, Halkier BA. CYP83b1 is the oxime-metabolizing enzyme in the glucosinolate pathway in *Arabidopsis*. J Biol Chem. 2001; 276:24790–24796. [PubMed: 11333274]
31. Dolan SK, O'Keeffe G, Jones GW, Doyle S. Resistance is not futile: gliotoxin biosynthesis, functionality and utility. Trends Microbiol. 2015; 23:419–428. [PubMed: 25766143]
32. Welch TR, Williams RM. Epidithiodioxopiperazines occurrence, synthesis and biogenesis. Nat Prod Rep. 2014; 31:1376–1404. [PubMed: 24816491]
33. Hidese R, Mihara H, Esaki N. Bacterial cysteine desulfurases: versatile key players in biosynthetic pathways of sulfur-containing biofactors. Appl Microbiol Biotechnol. 2011; 91:47–61. [PubMed: 21603932]
34. Dahl JU, Urban A, Bolte A, Sriyabhaya P, Donahue JL, Nimtz M, Larson TJ, Leimkuhler S. The identification of a novel protein involved in molybdenum cofactor biosynthesis in *Escherichia coli*. J Biol Chem. 2011; 286:35801–35812. [PubMed: 21856748]
35. Webb ME, Marquet A, Mendel RR, Rebeille F, Smith AG. Elucidating biosynthetic pathways for vitamins and cofactors. Nat Prod Rep. 2007; 24:988–1008. [PubMed: 17898894]
36. Cavuzic M, Liu Y. Biosynthesis of sulfur-containing tRNA modifications: A comparison of bacterial, archaeal, and eukaryotic pathways. Biomolecules. 2017; 7:27.
37. Sasaki E, Zhang X, Sun HG, Lu MY, Liu TL, Ou A, Li JY, Chen YH, Ealick SE, Liu HW. Co-opting sulphur-carrier proteins from primary metabolic pathways for 2-thiosugar biosynthesis. Nature. 2014; 510:427–431. [PubMed: 24814342]
38. Matthijs S, Baysse C, Koedam N, Tehrani KA, Verheyden L, Budzikiewicz H, Schafer M, Hoorelbeke B, Meyer JM, De Greve H, Cornelis P. The *Pseudomonas* siderophore quinolobactin is synthesized from xanthurenic acid, an intermediate of the kynurenine pathway. Mol Microbiol. 2004; 52:371–384. [PubMed: 15066027]
39. Godert AM, Jin M, McLafferty FW, Begley TP. Biosynthesis of the thioquinolobactin siderophore: an interesting variation on sulfur transfer. J Bacteriol. 2007; 189:2941–2944. [PubMed: 17209031]

40. Tang X, Li J, Millan-Aguinaga N, Zhang JJ, O'Neill EC, Ugalde JA, Jensen PR, Mantovani SM, Moore BS. Identification of thiotetronic acid antibiotic biosynthetic pathways by target-directed genome mining. ACS Chem Biol. 2015; 10:2841–2849. [PubMed: 26458099]
41. Yurkovich ME, Jenkins R, Sun Y, Tosin M, Leadlay PF. The polyketide backbone of thiolactomycin is assembled by an unusual iterative polyketide synthase. Chem Commun. 2017; 53:2182–2185.
42. Tao W, Yurkovich ME, Wen S, Lebe KE, Samborskyy M, Liu Y, Yang A, Liu Y, Ju Y, Deng Z, Tosin M, Sun Y, Leadlay PF. A genomics-led approach to deciphering the mechanism of thiotetronate antibiotic biosynthesis. Chem Sci. 2016; 7:376–385. [PubMed: 28791099]
43. Coyne S, Chizzali C, Khalil MN, Litomska A, Richter K, Beerhues L, Hertweck C. Biosynthesis of the antimetabolite 6-thioguanine in *Erwinia amylovora* plays a key role in fire blight pathogenesis. Angew Chem, Int Ed. 2013; 52:10564–10568.
44. Numata T, Ikeuchi Y, Fukai S, Suzuki T, Nureki O. Snapshots of tRNA sulphuration via an adenylated intermediate. Nature. 2006; 442:419–424. [PubMed: 16871210]
45. Sasaki E, Liu HW. Mechanistic studies of the biosynthesis of 2-thiosugar: evidence for the formation of an enzyme-bound 2-ketohexose intermediate in BexX-catalyzed reaction. J Am Chem Soc. 2010; 132:15544–15546. [PubMed: 20961106]
46. Broderick JB, Duffus BR, Duschene KS, Shepard EM. Radical *S*-adenosylmethionine enzymes. Chem Rev. 2014; 114:4229–4317. [PubMed: 24476342]
47. Lanz ND, Booker SJ. Identification and function of auxiliary iron–sulfur clusters in radical SAM enzymes. Biochim Biophys Acta, Proteins Proteomics. 2012; 1824:1196–1212.
48. McCarthy EL, Booker SJ. Destruction and reformation of an iron-sulfur cluster during catalysis by lipoyl synthase. Science. 2017; 358:373–377. [PubMed: 29051382]
49. Fluhe L, Marahiel MA. Radical *S*-adenosylmethionine enzyme catalyzed thioether bond formation in sactipeptide biosynthesis. Curr Opin Chem Biol. 2013; 17:605–612. [PubMed: 23891473]
50. Bruender NA, Wilcoxen J, Britt RD, Bandarian V. Biochemical and spectroscopic characterization of a radical *S*-adenosyl-L-methionine enzyme involved in the formation of a peptide thioether cross-link. Biochemistry. 2016; 55:2122–2134. [PubMed: 27007615]
51. Fluhe L, Knappe TA, Gattner MJ, Schafer A, Burghaus O, Linne U, Marahiel MA. The radical SAM enzyme AlbA catalyzes thioether bond formation in subtilosin A. Nat Chem Biol. 2012; 8:350–357. [PubMed: 22366720]
52. Fluhe L, Burghaus O, Wieckowski BM, Giessen TW, Linne U, Marahiel MA. Two [4Fe-4S] clusters containing radical SAM enzyme SkfB catalyze thioether bond formation during the maturation of the sporulation killing factor. J Am Chem Soc. 2013; 135:959–962. [PubMed: 23282011]
53. Wieckowski BM, Hegemann JD, Mielcarek A, Boss L, Burghaus O, Marahiel MA. The PqqD homologous domain of the radical SAM enzyme ThnB is required for thioether bond formation during thurincin H maturation. FEBS Lett. 2015; 589:1802–1806. [PubMed: 26026269]
54. Benjdia A, Guillot A, Lefranc B, Vaudry H, Leprince J, Berteau O. Thioether bond formation by SPASM domain radical SAM enzymes: CαH-atom abstraction in subtilosin A biosynthesis. Chem Commun. 2016; 52:6249–6252.
55. Baldwin JE, Bradley M. Isopenicillin-*N* synthase -mechanistic studies. Chem Rev. 1990; 90:1079–1088.
56. Roach PL, Clifton IJ, Fulop V, Harlos K, Barton GJ, Hajdu J, Andersson I, Schofield CJ, Baldwin JE. Crystal structure of isopenicillin *N* synthase is the first from a new structural family of enzymes. Nature. 1995; 375:700–704. [PubMed: 7791906]
57. Tamanaha E, Zhang B, Guo Y, Chang W-c, Barr EW, Xing G, St Clair J, Ye S, Neese F, Bollinger JM Jr, Krebs C. Spectroscopic Evidence for the Two C–H-Cleaving Intermediates of Aspergillus nidulans Isopenicillin N Synthase. J Am Chem Soc. 2016; 138:8862–8874. [PubMed: 27193226]
58. Tanret C. Sur une base nouvelle retiree du seigle ergote, l'ergothioneine. C R Acad Sci. 1909; 149:222–224.
59. Genghof DS, Inamine E, Kovalenko V, Melville DB. Ergothioneine in microorganisms. J Biol Chem. 1956; 223:9–17. [PubMed: 13376573]

60. Genghof DS, Vandamme O. Biosynthesis of ergothioneine and hercynine by mycobacteria. J Bacteriol. 1964; 87:852–862. [PubMed: 14137624]
61. Genghof DS, Van Damme O. Biosynthesis of ergothioneine from endogenous hercynine in *Mycobacterium smegmatis*. J Bacteriol. 1968; 95:340–344. [PubMed: 5644441]
62. Heath H, Wildy J. Biosynthesis of ergothioneine. Nature. 1957; 179:196–197. [PubMed: 13400134]
63. Melville DB, Eich S, Ludwig ML. The biosynthesis of ergothioneine. J Biol Chem. 1957; 224:871–877. [PubMed: 13405916]
64. Heath H, Wildy J. The biosynthesis of ergothioneine and histidine by *Claviceps purpurea* I The incorporation of [2-^{14}C]-acetate. Biochem J. 1956; 64:612–620. [PubMed: 13382810]
65. Heath H, Wildy J. Biosynthesis of ergothioneine by *Claviceps purpurea* III The incorporation of labelled histidine. Biochem J. 1958; 68:407–410. [PubMed: 13522637]
66. Askari A, Melville DB. The reaction sequence in ergothioneine biosynthesis: hercynine as an intermediate. J Biol Chem. 1962; 237:1615–1618. [PubMed: 13862898]
67. Reinhold VN, Ishikawa Y, Melville DB. Conversion of histidine to hercynine by *Neurospora crassa*. J Bacteriol. 1970; 101:881–884. [PubMed: 5438052]
68. Ishikawa Y, Melville DB. The enzymatic a-N-methylation of histidine. J Biol Chem. 1970; 245:5967–5973. [PubMed: 5484456]
69. Ishikawa Y, Israel SE, Melville DB. Participation of an intermediate sulfoxide in the enzymatic thiolation of the imidazole ring of hercynine to form ergothioneine. J Biol Chem. 1974; 249:4420–4427. [PubMed: 4276459]
70. Hu W, Song H, Sae Her A, Bak DW, Naowarojna N, Elliott SJ, Qin L, Chen X, Liu P. Bioinformatic and biochemical characterizations of C-S bond formation and cleavage enzymes in the fungus *Neurospora crassa* ergothioneine biosynthetic pathway. Org Lett. 2014; 16:5382–5385. [PubMed: 25275953]
71. Shapiro BM, Hopkins PB. Ovothiols: biological and chemical perspectives. Adv Enzymol Relat Areas Mol Biol. 2006; 64:291–316.
72. Spies HS, Steenkamp DJ. Thiols of intracellular pathogens. Identification of ovothiol A in *Leishmania donovani* and structural analysis of a novel thiol from *Mycobacterium bovis*. Eur J Biochem. 1994; 224:203–213. [PubMed: 8076641]
73. Steenkamp DJ, Spies HS. Identification of a major low-molecular-mass thiol of the trypanosomatid *Crithidia fasciculata* as ovothiol A. Facile isolation and structural analysis of the bimane derivative. Eur J Biochem. 1994; 223:43–50. [PubMed: 8033907]
74. Steenkamp DJ, Weldrick D, Spies HS. Studies on the biosynthesis of ovothiol A. Eur J Biochem. 1996; 242:557–566. [PubMed: 9022682]
75. Vogt RN, Spies HS, Steenkamp DJ. The biosynthesis of ovothiol A (N-methyl-4-mercaptohistidine). Identification of S-(4′-L-histidyl)-L-cysteine sulfoxide as an intermediate and the products of the sulfoxide lyase reaction. Eur J Biochem. 2001; 268:5229–5241. [PubMed: 11606184]
76. Braunshausen A, Seebeck FP. Identification and characterization of the first ovothiol biosynthetic enzyme. J Am Chem Soc. 2011; 133:1757–1759. [PubMed: 21247153]
77. Seebeck FP. *In vitro* reconstitution of mycobacterial ergothioneine biosynthesis. J Am Chem Soc. 2010; 132:6632–6633. [PubMed: 20420449]
78. Vit A, Misson L, Blankenfeldt W, Seebeck FP. Ergothioneine biosynthetic methyltransferase EgtD reveals the structural basis of aromatic amino acid betaine biosynthesis. ChemBioChem. 2015; 16:119–125. [PubMed: 25404173]
79. Song H, Hu W, Naowarojna N, Her AS, Wang S, Desai R, Qin L, Chen X, Liu P. Mechanistic studies of a novel C-S lyase in ergothioneine biosynthesis: the involvement of a sulfenic acid intermediate. Sci Rep. 2015; 5:11870. [PubMed: 26149121]
80. Irani S, Naowarojna N, Tang Y, Kathuria KR, Wang S, Dhembi A, Lee N, Yan W, Lyu H, Costello CE, Liu P, Zhang YJ. Snapshots of CS Cleavage in Egt2 Reveals Substrate Specificity and Reaction Mechanism. Cell Chem Biol. 2018; doi: 10.1016/j.chembiol.2018.02.002
81. Bello MH, Barrera-Perez V, Morin D, Epstein L. The *Neurospora crassa* mutant NcΔEgt-1 identifies an ergothioneine biosynthetic gene and demonstrates that ergothioneine enhances

conidial survival and protects against peroxide toxicity during conidial germination. Fungal Genet Biol. 2012; 49:160–172. [PubMed: 22209968]

82. Sheridan KJ, Lechner BE, O'Keeffe G, Keller MA, Werner ER, Lindner H, Jones GW, Haas H, Doyle S. Ergothioneine biosynthesis and functionality in the opportunistic fungal pathogen, *Aspergillus fumigatus*. Sci Rep. 2016; 6:35306. [PubMed: 27748436]
83. Pluskal T, Ueno M, Yanagida M. Genetic and metabolomic dissection of the ergothioneine and selenoneine biosynthetic pathway in the fission yeast, *S. pombe*, and construction of an overproduction system. PLoS One. 2014; 9:e97774. [PubMed: 24828577]
84. Jones GW, Doyle S, Fitzpatrick DA. The evolutionary history of the genes involved in the biosynthesis of the antioxidant ergothioneine. Gene. 2014; 549:161–170. [PubMed: 25068406]
85. Liao C, Seebeck FP. Convergent evolution of ergothioneine biosynthesis in cyanobacteria. ChemBioChem. 2017; 18:2115–2118. [PubMed: 28862368]
86. Song H, Leninger M, Lee N, Liu P. Regioselectivity of the oxidative C–S bond formation in ergothioneine and ovothiol biosyntheses. Org Lett. 2013; 15:4854–4857. [PubMed: 24016264]
87. Mashabela GT, Seebeck FP. Substrate specificity of an oxygen dependent sulfoxide synthase in ovothiol biosynthesis. Chem Commun. 2013; 49:7714–7716.
88. Joseph CA, Maroney MJ. Cysteine dioxygenase: structure and mechanism. Chem Commun. 2007:3338–3349.
89. Burn R, Misson L, Meury M, Seebeck FP. Anaerobic origin of ergothioneine. Angew Chem, Int Ed. 2017; 56:12508–12511.
90. Cheah IK, Halliwell B. Ergothioneine; antioxidant potential, physiological function and role in disease. Biochim Biophys Acta, Mol Basis Dis. 2012; 1822:784–793.
91. Ruszczycky MW, Liu HW. The surprising history of an antioxidant. Nature. 2017; 551:37–38. [PubMed: 29094692]
92. Goncharenko KV, Vit A, Blankenfeldt W, Seebeck FP. Structure of the sulfoxide synthase EgtB from the ergothioneine biosynthetic pathway. Angew Chem, Int Ed. 2015; 54:2821–2824.
93. Goncharenko KV, Seebeck FP. Conversion of a non-heme iron-dependent sulfoxide synthase into a thiol dioxygenase by a single point mutation. Chem Commun. 2016; 52:1945–1948.
94. Li W, Pierce BS. Steady-state substrate specificity and O_2-coupling efficiency of mouse cysteine dioxygenase. Arch Biochem Biophys. 2015; 565:49–56. [PubMed: 25444857]
95. Song H, Her AS, Raso F, Zhen Z, Huo Y, Liu P. Cysteine oxidation reactions catalyzed by a mononuclear non-heme iron enzyme (OvoA) in ovothiol biosynthesis. Org Lett. 2014; 16:2122–2125. [PubMed: 24684381]
96. Kumar D, Thiel W, de Visser SP. Theoretical study on the mechanism of the oxygen activation process in cysteine dioxygenase enzymes. J Am Chem Soc. 2011; 133:3869–3882. [PubMed: 21344861]
97. Aluri S, de Visser SP. The mechanism of cysteine oxygenation by cysteine dioxygenase enzymes. J Am Chem Soc. 2007; 129:14846–14847. [PubMed: 17994747]
98. Faponle AS, Seebeck FP, de Visser SP. Sulfoxide synthase versus cysteine dioxygenase reactivity in a nonheme iron enzyme. J Am Chem Soc. 2017; 139:9259–9270. [PubMed: 28602090]
99. Wei WJ, Siegbahn PE, Liao RZ. Theoretical study of the mechanism of the non-heme iron enzyme EgtB. Inorg Chem. 2017; 56:3589–3599. [PubMed: 28277674]
100. Chen L, Naowarojna N, Song H, Wang S, Wang J, Deng Z, Zhao C, Liu P. Use of a tyrosine analog to modulate the two activities of a non-heme iron enzyme OvoA in ovothiol biosynthesis, cysteine oxidation versus oxidative C-S bond formation. J Am Chem Soc. 2018; :4604–4612. DOI: 10.1021/jacs.7b13628 [PubMed: 29544051]
101. Yang J, Yan R, Roy A, Xu D, Poisson J, Zhang Y. The I-TASSER Suite: protein structure and function prediction. Nat Methods. 2015; 12:7. [PubMed: 25549265]
102. Simmons CR, Liu Q, Huang Q, Hao Q, Begley TP, Karplus PA, Stipanuk MH. Crystal structure of mammalian cysteine dioxygenase. A novel mononuclear iron center for cysteine thiol oxidation. J Biol Chem. 2006; 281:18723–18733. [PubMed: 16611640]

103. McCoy JG, Bailey LJ, Bitto E, Bingman CA, Aceti DJ, Fox BG, Phillips GN. Structure and mechanism of mouse cysteine dioxygenase. Proc Natl Acad Sci U S A. 2006; 103:3084–3089. [PubMed: 16492780]
104. Ye S, Wu Xa, Wei L, Tang D, Sun P, Bartlam M, Rao Z. An insight into the mechanism of human cysteine dioxygenase. Key roles of the thioether-bonded tyrosine-cysteine cofactor. J Biol Chem. 2007; 282:3391–3402. [PubMed: 17135237]
105. Jacob C. A scent of therapy: pharmacological implications of natural products containing redox-active sulfur atoms. Nat Prod Rep. 2006; 23:851–863. [PubMed: 17119635]
106. Kuettner EB, Hilgenfeld R, Weiss MS. The active principle of garlic at atomic resolution. J Biol Chem. 2002; 277:46402–46407. [PubMed: 12235163]
107. Melville DB, Horner WH, Lubschez R. Tissue ergothioneine. J Biol Chem. 1954; 206:221–228. [PubMed: 13130544]
108. Shires TK, Brummel MC, Pulido JS, Stegink LD. Ergothioneine distribution in bovine and porcine ocular tissues. Comp Biochem Physiol, Part C: Pharmacol, Toxicol Endocrinol. 1997; 117:117–120.
109. Leone E, Mann T. Ergothioneine in the seminal vesicle secretion. Nature. 1951; 168:205.
110. Grundemann D, Harlfinger S, Golz S, Geerts A, Lazar A, Berkels R, Jung N, Rubbert A, Schomig E. Discovery of the ergothioneine transporter. Proc Natl Acad Sci U S A. 2005; 102:5256–5261. [PubMed: 15795384]
111. Nakamura T, Yoshida K, Yabuuchi H, Maeda T, Tamai I. Functional characterization of ergothioneine transport by rat organic cation/carnitine transporter Octn1 (slc22a4). Biol Pharm Bull. 2008; 31:1580–1584. [PubMed: 18670092]
112. Taubert D, Jung N, Goeser T, Schömig E. Increased ergothioneine tissue concentrations in carriers of the Crohn's disease risk-associated 503F variant of the organic cation transporter OCTN1. Gut. 2009; 58:312–314. [PubMed: 19136526]
113. Grigat S, Harlfinger S, Pal S, Striebinger R, Golz S, Geerts A, Lazar A, Schömig E, Gründemann D. Probing the substrate specificity of the ergothioneine transporter with methimazole, hercynine, and organic cations. Biochem Pharmacol. 2007; 74:309–316. [PubMed: 17532304]
114. Kato Y, Kubo Y, Iwata D, Kato S, Sudo T, Sugiura T, Kagaya T, Wakayama T, Hirayama A, Sugimoto M, Sugihara K, Kaneko S, Soga T, Asano M, Tomita M, Matsui T, Wada M, Tsuji A. Gene knockout and metabolome analysis of carnitine/organic cation transporter OCTN1. Pharm Res. 2010; 27:832–840. [PubMed: 20224991]
115. Paul B, Snyder S. The unusual amino acid L-ergothioneine is a physiologic cytoprotectant. Cell Death Differ. 2010; 17:1134. [PubMed: 19911007]
116. Hartman PE. Ergothioneine as antioxidant. Methods Enzymol. 1990; 186:310–318. [PubMed: 2172707]
117. Hand CE, Taylor NJ, Honek JF. *Ab initio* studies of the properties of intracellular thiols ergothioneine and ovothiol. Bioorg Med Chem Lett. 2005; 15:1357–1360. [PubMed: 15713386]
118. Scott EM, Duncan IW, Ekstrand V. Purification and properties of glutathione reductase of human erythrocytes. J Biol Chem. 1963; 238:3928–3933. [PubMed: 14086726]
119. Taubert D, Lazar A, Grimberg G, Jung N, Rubbert A, Delank KS, Perniok A, Erdmann E, Schömig E. Association of rheumatoid arthritis with ergothioneine levels in red blood cells: a case control study. J Rheumatol. 2006; 33:2139–2145. [PubMed: 17086603]
120. Tokuhiro S, Yamada R, Chang X, Suzuki A, Kochi Y, Sawada T, Suzuki M, Nagasaki M, Ohtsuki M, Ono M, Furukawa H, Nagashima M, Yoshino S, Mabuchi A, Sekine A, Saito S, Takahashi A, Tsunoda T, Nakamura Y, Yamamoto K. An intronic SNP in a RUNX1 binding site of SLC22A4, encoding an organic cation transporter, is associated with rheumatoid arthritis. Nat Genet. 2003; 35:341–348. [PubMed: 14608356]
121. Peltekova VD, Wintle RF, Rubin LA, Amos CI, Huang Q, Gu X, Newman B, Van Oene M, Cescon D, Greenberg G, Griffiths AM, St George-Hyslop PH, Siminovitch KA. Functional variants of OCTN cation transporter genes are associated with Crohn disease. Nat Genet. 2004; 36:471–475. [PubMed: 15107849]

122. Leung E, Hong J, Fraser AG, Merriman TR, Vishnu P, Krissansen GW. Polymorphisms in the organic cation transporter genes SLC22A4 and SLC22A5 and Crohn's disease in a New Zealand Caucasian cohort. Immunol Cell Biol. 2006; 84:233–236. [PubMed: 16519742]

123. Kaneko I, Takeuchi Y, Yamaoka Y, Tanaka Y, Fukuda T, Fukumori Y, Mayumi T, Hama T. Quantitative determination of ergothioneine in plasma and tissues by TLC-densitometry. Chem Pharm Bull. 1980; 28:3093–3097. [PubMed: 7448946]

124. Briggs I. Ergothioneine in the central nervous system. J Neurochem. 1972; 19:27–35. [PubMed: 4400394]

125. Crossland J, Mitchell J, Woodruff GN. The presence of ergothioneine in the central nervous system and its probable identity with the cerebellar factor. J Physiol. 1966; 182:427–438. [PubMed: 5942036]

126. Moncaster JA, Walsh DT, Gentleman SM, Jen LS, Aruoma OI. Ergothioneine treatment protects neurons against N-methyl-D-aspartate excitotoxicity in an *in vivo* rat retinal model. Neurosci Lett. 2002; 328:55–59. [PubMed: 12123858]

127. Libby P, Ridker PM, Hansson GK. Progress and challenges in translating the biology of atherosclerosis. Nature. 2011; 473:317–325. [PubMed: 21593864]

128. Bastard JP, Maachi M, Van Nhieu JT, Jardel C, Bruckert E, Grimaldi A, Robert JJ, Capeau J, Hainque B. Adipose tissue IL-6 content correlates with resistance to insulin activation of glucose uptake both in vivo and in vitro. J Clin Endocrinol Metab. 2002; 87:2084–2089. [PubMed: 11994345]

129. Lafon-Cazal M, Pietri S, Culcasi M, Bockaert J. NMDA-dependent superoxide production and neurotoxicity. Nature. 1993; 364:535. [PubMed: 7687749]

130. Martin KR. The bioactive agent ergothioneine, a key component of dietary mushrooms, inhibits monocyte binding to endothelial cells characteristic of early cardiovascular disease. J Med Food. 2010; 13:1340–1346. [PubMed: 21091247]

131. Zhao Q, Wang M, Xu D, Zhang Q, Liu W. Metabolic coupling of two small-molecule thiols programs the biosynthesis of lincomycin A. Nature. 2015; 518:115. [PubMed: 25607359]

132. Newton GL, Leung SS, Wakabayashi JI, Rawat M, Fahey RC. The DinB superfamily includes novel mycothiol, bacillithiol, and glutathione *S*-transferases. Biochemistry. 2011; 50:10751–10760. [PubMed: 22059487]

133. Rawat M, Av-Gay Y. Mycothiol-dependent proteins in actinomycetes. FEMS Microbiol Rev. 2007; 31:278–292. [PubMed: 17286835]

134. Jothivasan VK, Hamilton CJ. Mycothiol: synthesis, biosynthesis and biological functions of the major low molecular weight thiol in actinomycetes. Nat Prod Rep. 2008; 25:1091–1117. [PubMed: 19030604]

135. Komatsu W, Miura Y, Yagasaki K. Suppression of hypercholesterolemia in hepatoma-bearing rats by cabbage extract and its component, *S*-methyl-L-cysteine sulfoxide. Lipids. 1998; 33:499–503. [PubMed: 9625597]

136. Augusti KT, Sheela CG. Antiperoxide effect of S-allyl cysteine sulfoxide, an insulin secretagogue, in diabetic rats. Experientia. 1996; 52:115–119. [PubMed: 8608811]

137. Kodama H, Zhang J, Sugahara K. Novel priming compounds of cystathionine metabolites on superoxide generation in human neutrophils. Biochem Biophys Res Commun. 2000; 269:297–301. [PubMed: 10708546]

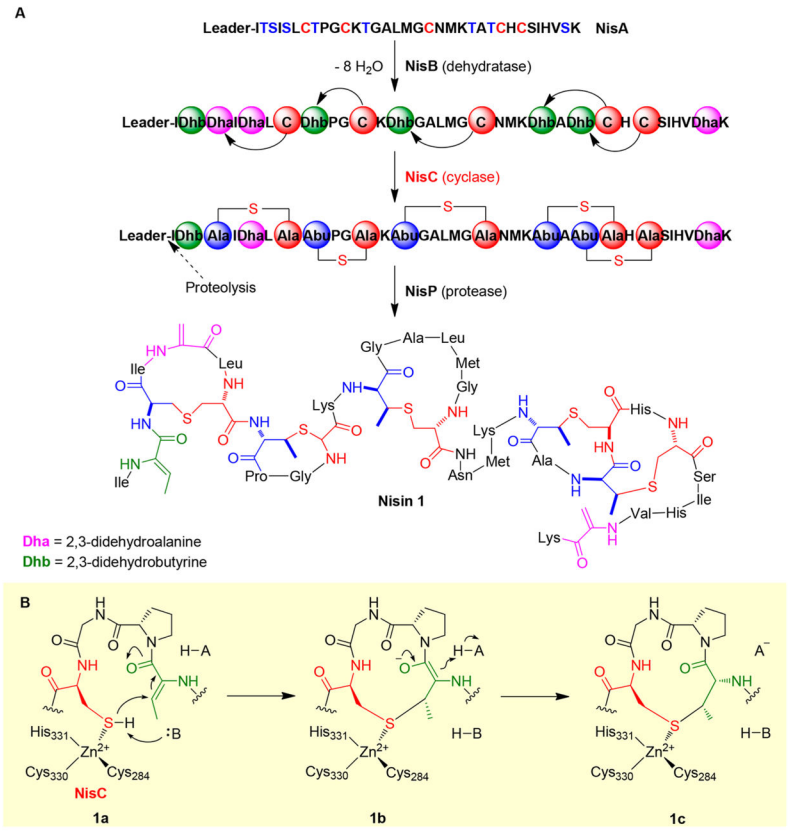

Figure 1.

Ionic type of C–S bond formation in nisin biosynthesis. (A) Overall biosynthetic pathway of nisin. (B) NisC activates the cysteine thiol by coordinating to a Zn^{2+} ion, allowing nucleophilic attacks of the Dhb or Dha β-carbon position to give a thioether linkage.

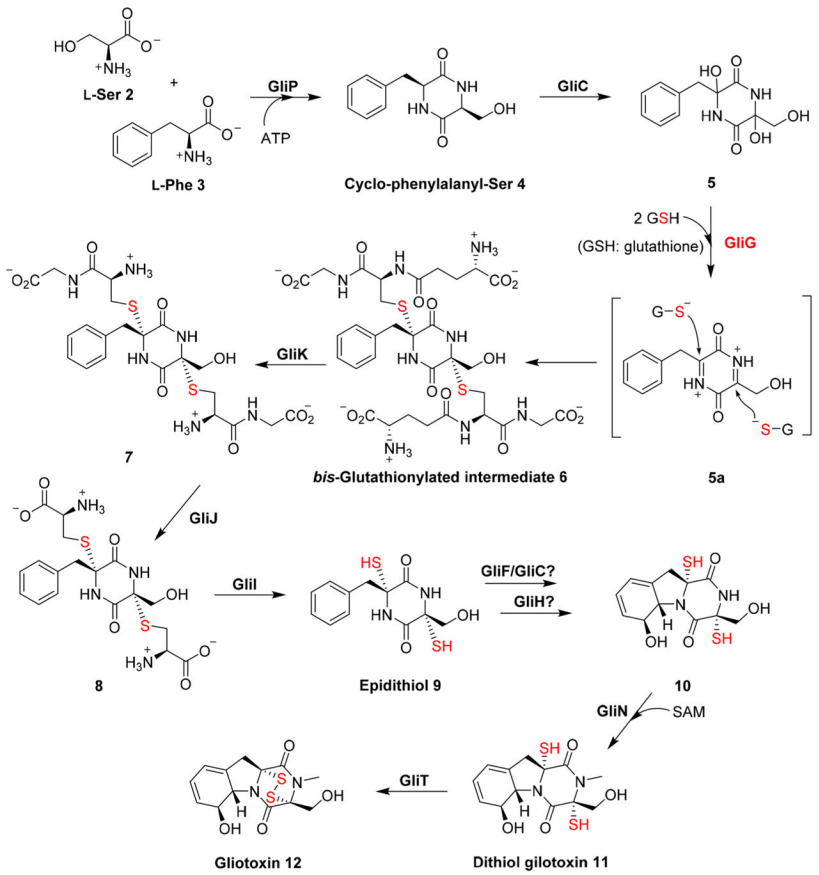

Figure 2.

C–S bond formation through an ionic type of reaction in gliotoxin biosynthesis. In the gliotoxin **12** biosynthetic pathway, C–S bond formation mediated by GliG undergoes a nucleophilic attack by GSH on an acyliminium intermediate **5a**, giving bis-glutathionylated intermediate **6**.

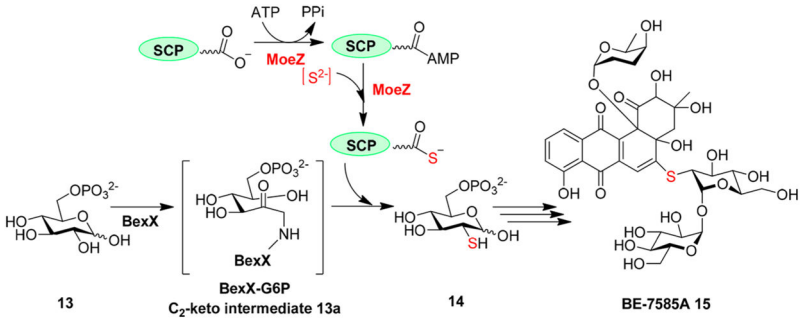

Figure 3.

Sulfur-delivery machinery in BE-7585A biosynthesis. MoeZ not only activates the C-terminus of a sulfur carrier protein (SCP) using ATP but also mediates the transfer of the sulfur to the activated SCP to form a thiocarboxylate. The activated SCP then incorporates sulfur into BexX–substrate complex **13a** to produce **14**.

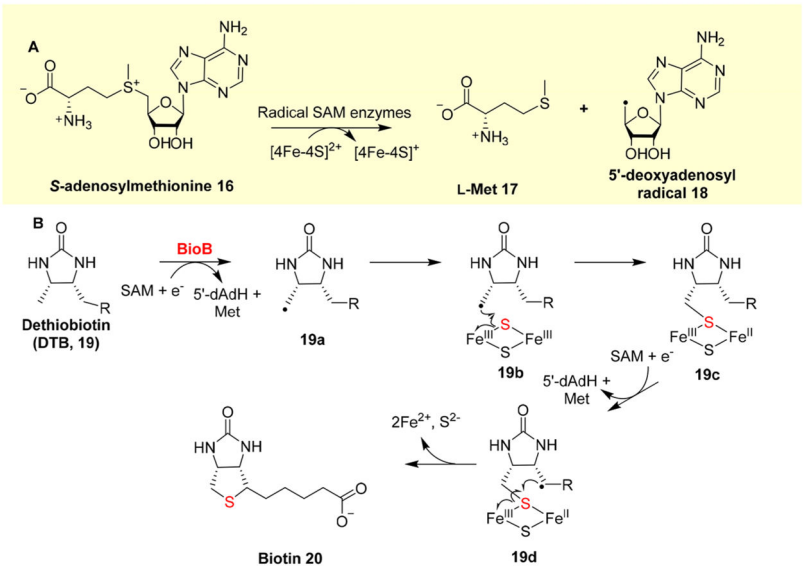

Figure 4.

Radical type of sulfur insertion mechanism (BioB catalysis of biotin biosynthesis). (A) Reductive cleavage of SAM. (B) Proposed BioB catalytic mechanism in which thioether bond formation goes through two substrate-based radical intermediates, **19a** and **19d**.

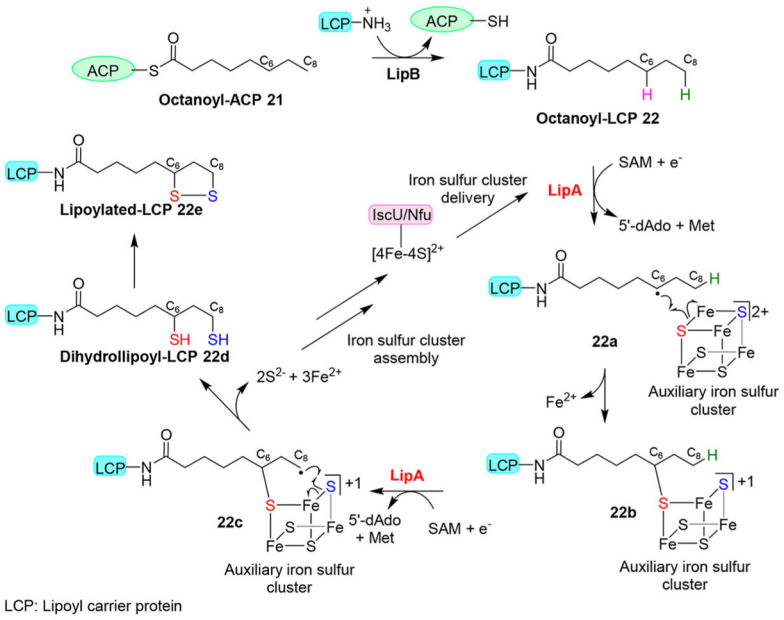

Figure 5.

Proposed lipoic acid biosynthetic mechanism. In lipoic acid biosynthesis, a radical SAM enzyme LipA mediates the transfer of sulfurs from an auxiliary [4Fe-4S] cluster to octanoyl-LCP substrate **22**. The auxiliary [4Fe-4S] cluster is then replenished for the next cycle by the iron–sulfur cluster maturation system, e.g., iron–sulfur cluster delivered by IscU or Nfu protein.

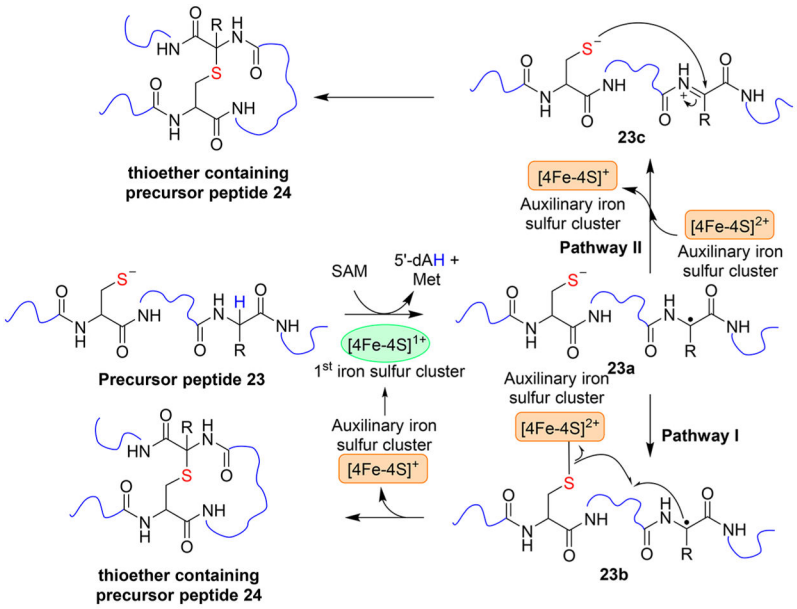

Figure 6.

Proposed mechanistic models of Alba, which catalyzes sactipeptide thioether linkage formation in the biosynthesis of subtilosin A. The first [4Fe-4S] cluster undergoes reductive cleavage of SAM. The role of the auxiliary cluster is not yet clear.

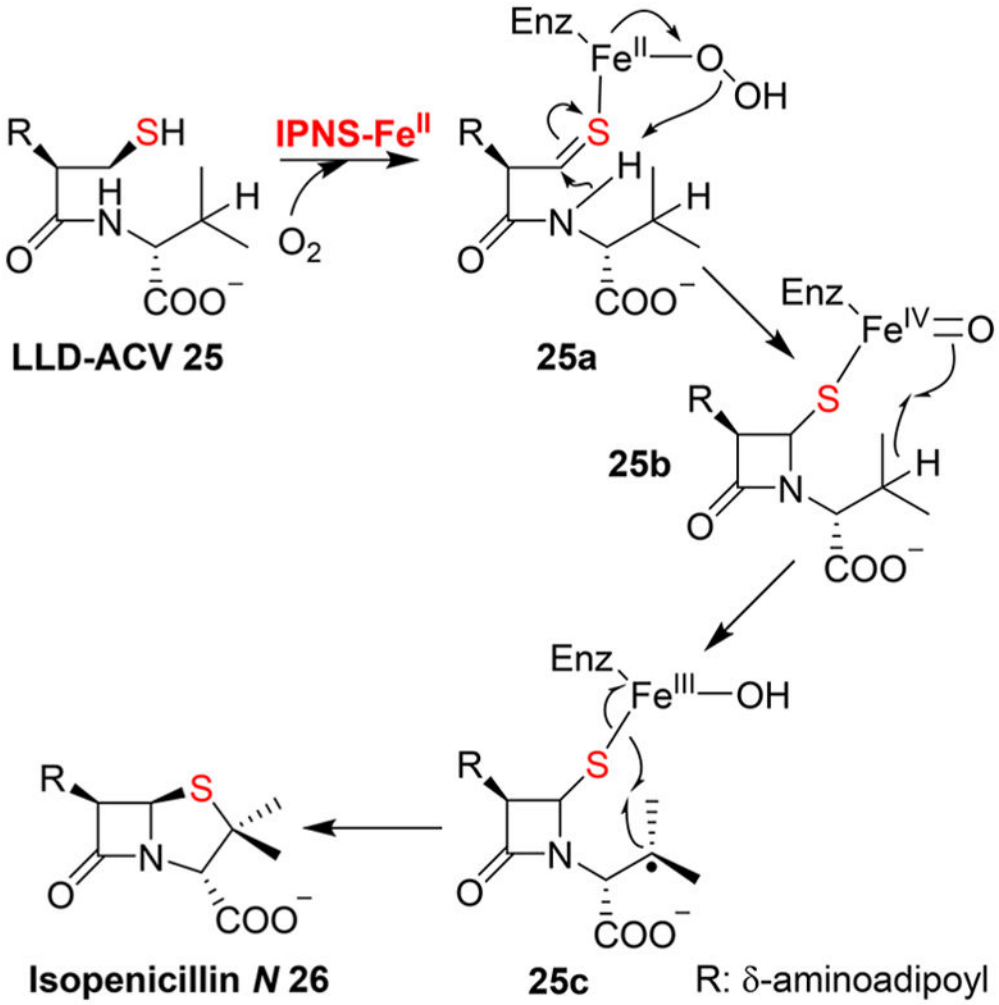

Figure 7.

Proposed mechanistic model of IPNS that involves two stages:β-lactam **25b** formation followed by thiazolidine ring formation (**25c** → **26**) through an Fe^{IV}═O species **25b**.

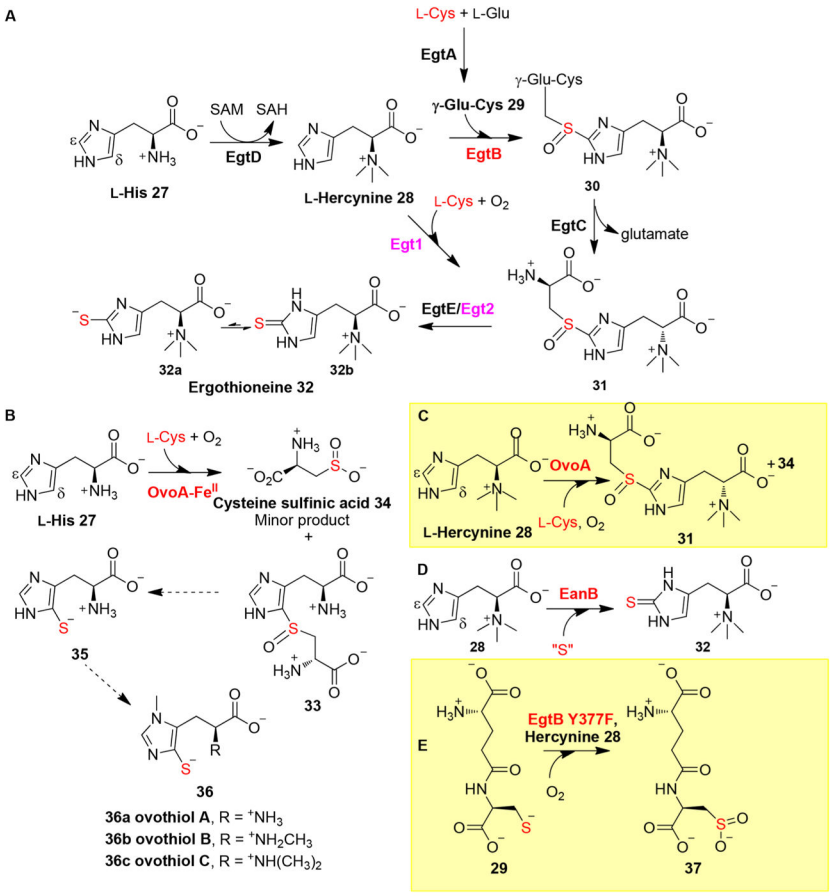

Figure 8.

Ergothioneine and ovothiol biosynthetic pathways. (A) Two aerobic ergothioneine biosynthetic pathways. (B) Proposed biosynthetic pathway of ovothiols. (C) OvoA reaction when hercynine **28** was used as the substrate, where OvoA changes its regioselectivity to the Egt1 type. (D) Anaerobic ergothioneine biosynthetic pathway, in which sulfur is incorporated at the ε-position of the hercynine imidazole ring by a rhodanese, EanB. (E) Dominant reaction of the EgtB Y377F mutant.

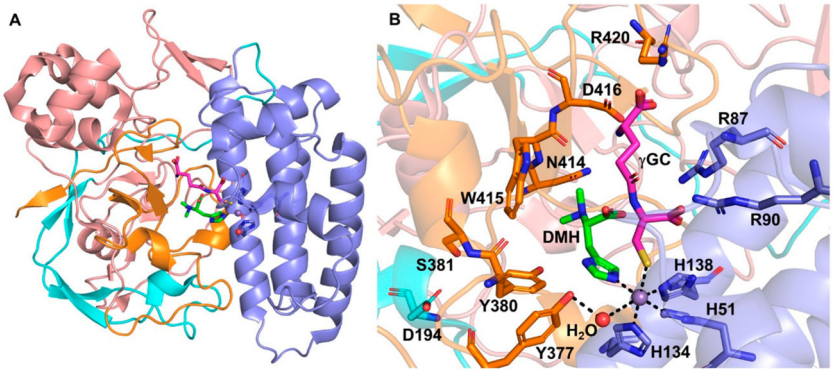

Figure 9.

M. thermoresistible EgtB structure. (A) Overall EgtB topology showing the N-terminus with a DinB-like helix bundle (blue) with the C-terminus containing a lectin fold (salmon/orange). EgtB contains a two-stranded β-sheet region (cyan). (B) EgtB tertiary complex with dimethylhistidine (DMH, green sticks) and γ-glutamyl-cysteine (γGC, magenta sticks) as the ligands of the Mn^{2+} center (purple sphere), which is coordinated by H51, H134, and H138. Notably, the water ligand (red sphere) also forms a hydrogen bond with active site Y377.

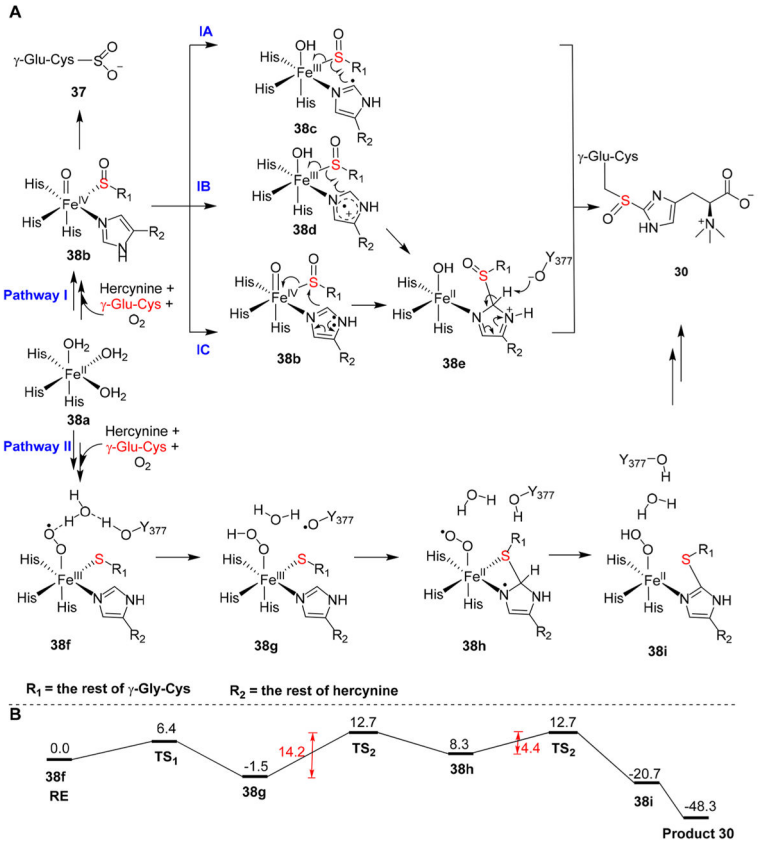

Figure 10.

Proposed mechanistic models for EgtB catalysis. (A) In pathway I, substrate binding and oxygen activation result in an Fe(III)–superoxo intermediate, which reacts with cysteine thiolate to form sulfenic acid and an Fe^{IV}═O species **38b**. In this pathway, Y377 is proposed to function as a general base. In pathway II, after oxygen activation, Fe^{III}–superoxo intermediate **38f** oxidizes Y337 by a proton-coupled electron transfer process to generate a tyrosyl radical **38g**. (B) Energy diagram of intermediates along pathway II in panel A based on quantum mechanics/molecular mechanics calculations.

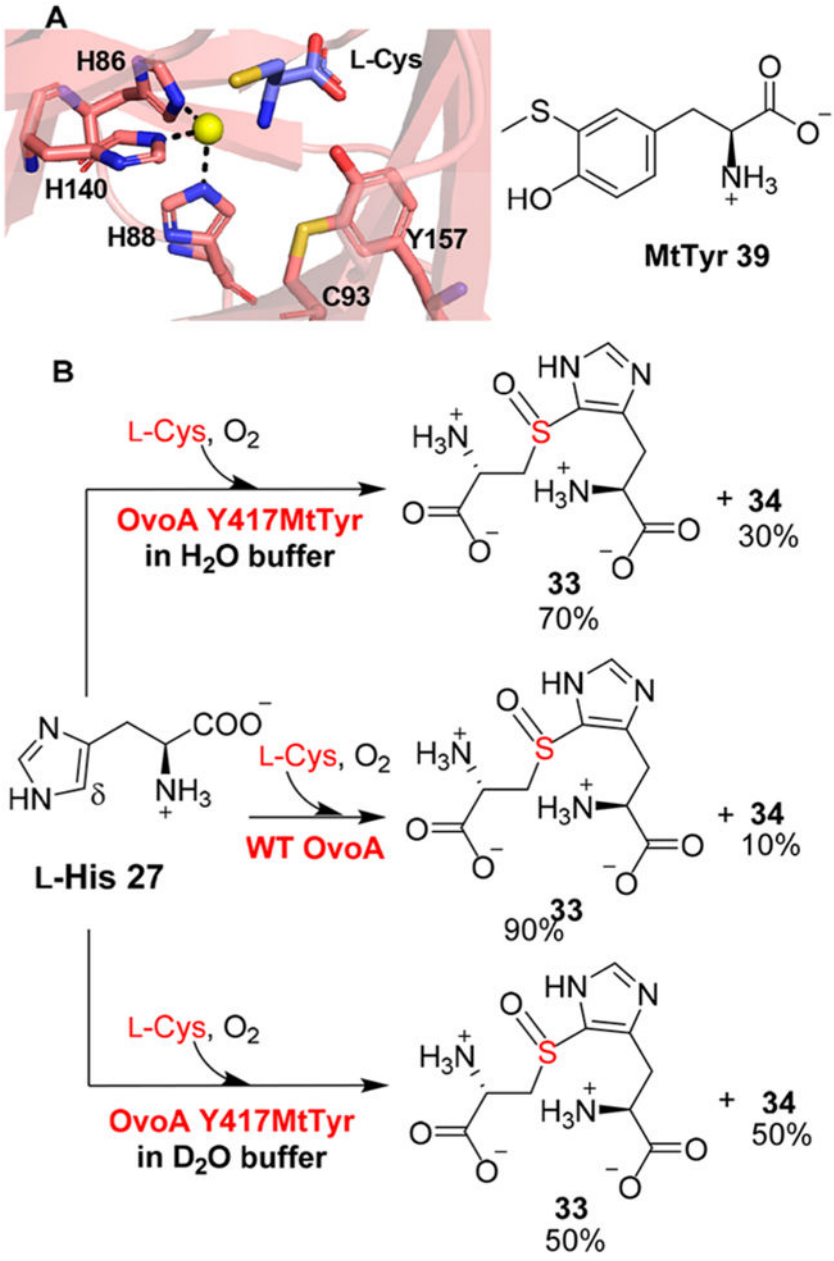

Figure 11.

Modulating OvoA reactivity by replacing Y417 using a tyrosine analogue. (A) The active site of the cysteine dioxygenase crystal structure shows the tyrosine–cysteine cross-link, which is mimicked by a tyrosine analogue MtTyr in the OvoA Y417MtTyr variant. (B) Reaction results for wild-type OvoA and the Y417MtTyr variant, suggesting that the OvoA activities can be modulated by replacing Y417 using tyrosine analogues.

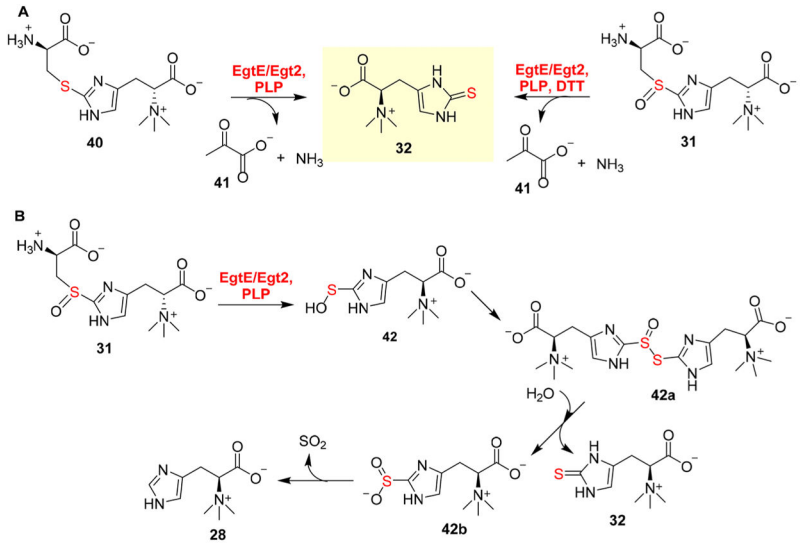

Figure 12.

EgtE/Egt2 reactions. (A) C–S lyase EgtE reactions using sulfoxide **31** as the substrate in the presence of reductants or thioether **40** as the substrate in the absence of reductants. (B) Mechanistic model for the reaction using sulfoxide **31** as the substrate in the absence of reductants, in which ergothioneine **32** and hercynine **28** are produced in a 1:1 ratio.

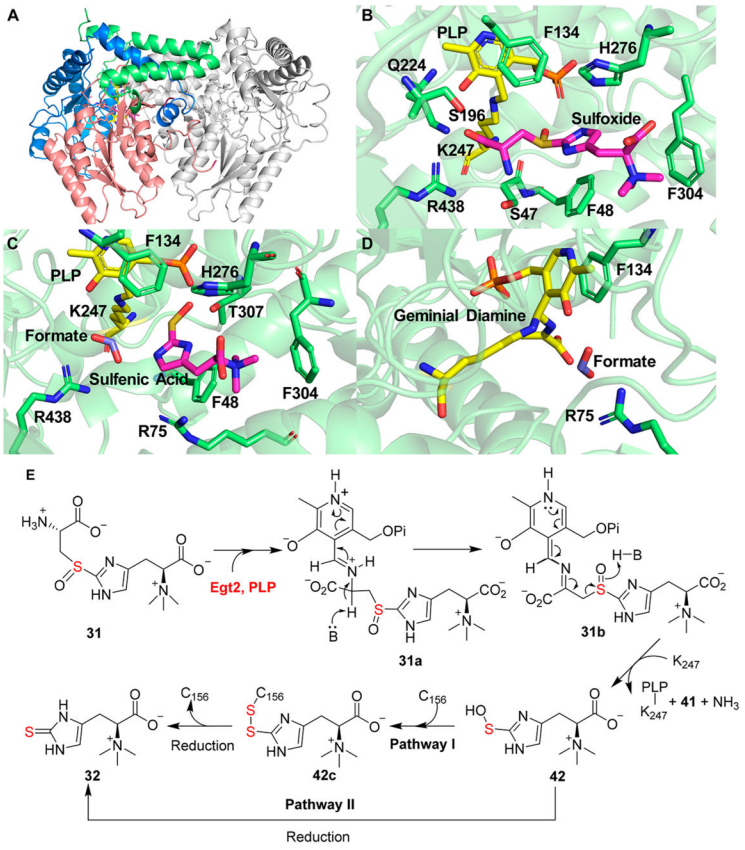

Figure 13.

Egt2 structure and our mechanistic model. (A) Overall structure of the Egt2 Y134F·substrate **31** binary complex in which the central catalytic domain is colored salmon. (B) Active site of the Egt2 Y134F·substrate **31** binary complex (sulfoxide **31** shown as magenta sticks and the PLP cofactor as yellow sticks). (C) Interactions between the active site residues and ergothioneine sulfenic acid intermediate **42** (shown as magenta sticks). (D) Aminoacrylate germinal diamine intermediate (shown as yellow sticks). (E) Proposed Egt2 mechanistic model. Sulfenic acid intermediate **42** could be trapped by C156 at the exit of the active site (pathway I) or be reduced directly (pathway II) to ergothioneine by reductants after it is released from the active site.

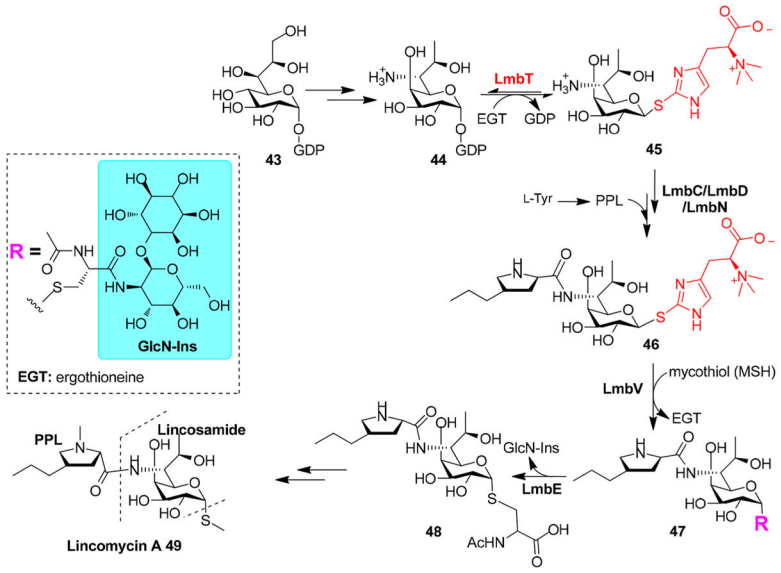

Figure 14.

Lincomycin A biosynthesis shows the involvement of two small molecular thiols, ergothioneine (EGT) and mycothiol (MSH).